Continuous and Short Fiber Reinforced Composites:

Optical Coherence Tomography and Mechanical Characterization

Sanaz Saadat

A dissertation submitted in partial fulfillment of the requirements for the degree
of
Doctor of Philosophy

University of Washington

2026

Committee:

Alireza Sadr, Chair

Daniel Chan

Kwok-Hung Chung

Robert Cornell

Frank Roberts, GSR

Program Authorized to Offer Degree:

Department of Oral Health Sciences

University of Washington

Abstract

Continuous and Short Fiber Reinforced Composites:
Optical Coherence Tomography and Mechanical Characterization

Sanaz Saadat

Chair of the Supervisory Committee:
Alireza Sadr

Department of Oral Health Sciences

Optimizing polymerization behavior and mechanical performance remains a major challenge in dental composite restorations. This research investigates the effects of short fiber and continuous fiber reinforcement on polymerization behavior and flexural strength. Real-time Optical Coherence Tomography (OCT) imaging of deep Class I restorations revealed that continuous fiber reinforcement reduced polymerization shrinkage induced gap formation, with the greatest effect observed in conventional composite formulations. Flexural strength 3-points bending test further emphasized that combining short-fiber reinforced composites with the continuous fiber achieved higher strength and exhibited more favorable, less catastrophic failure patterns than conventional composites. Overall, the incorporation of continuous fiber increased both the flexural strength and deformation capacity of the tested composite systems, and combined use of short and continuous fibers improved interfacial adaptation, lowered shrinkage stress, and enhanced overall structural performance, supporting continuous fiber reinforcement as an effective approach for increasing the durability of composite restorations.

Table of Contents

Acknowledgments

This body of work would not have been possible without the contributions, guidance, and support of many individuals and sources. I would like to extend my sincere appreciation to the University of Washington School of Dentistry, particularly the Department of Oral Health Sciences, for providing the academic environment, resources, and support that made this work possible. The department's commitment to excellence in research and education has been fundamental to my growth and development throughout this program.

My profound appreciation goes to my mentor, Dr. Alireza Sadr, for generously sharing his knowledge and for being a caring, patient, and truly dedicated mentor. Working in a field that is a less-traveled path, I have been especially fortunate to learn from someone who is not only deeply knowledgeable but also recognized as one of the leading experts in this area. His guidance, thoughtful mentorship, and kind spirit have shaped both my research and my development as a scholar. I am deeply thankful for his unwavering support and for the invaluable insight he has provided throughout this journey.

I would also like to extend my heartfelt appreciation to my program director, Dr. Robert Cornell, whose genuine care for students and commitment to their success have made a profound impact on my academic journey. He is widely known for his big heart, his thoughtful guidance, and the innovative study methods he has suggested that have proven remarkably effective, shaping the way many of us learn. His willingness to invest time, energy, and personal attention into each student reflects a level of dedication that is truly exceptional. I am deeply grateful for his support and for the positive, lasting influence he has had on my education and academic journey.

My committee has provided invaluable mentoring, and I would not have been able to accomplish this without their expertise and support. My sincere thanks go to Dr. Albert Chung, whose kindness and generosity were truly appreciated. He took the time to help explore testing options, guide me through sample fabrication, and assist in locating testing sites across campus. His support and expertise played an important role in the development of the flexural strength study.

I am sincerely grateful to Dr. Daniel C. N. Chan and Dr. Frank Roberts for their guidance, support, and valuable insights during my academic progress and for their generous time, thoughtful coaching, and continual support in shaping my proposal and research. Their mentorship has been an essential part of shaping my scholarly path.

My sincere appreciation also goes to Dr. John Sorensen for kindly providing access to Instron machines and for his thoughtful guidance and scientific advice during the course of flexural strength studies. Also, to Dr. Hideo Kakuma of Yoshida Dental for generously providing the OCT system. Their contributions and support played a huge role in the successful completion of this work. I am especially grateful to Dr. Grant Chyz for his valuable assistance in fabricating the jig and specimens used in the flexural strength study, as well as for his insightful suggestion on how to incorporate Ribbond. and to Dr. Nafiseh Najmafshar for her assistance in specimen preparation. I gratefully acknowledge Jeremy Rudo (Ribbond) for generously providing the Ribbond material used in this research and Dr. David Rudo for his insights and valuable advice with the literature review.

I would like to express my sincere appreciation to Lora Brewsaugh for her valuable administrative support throughout my academic journey. Her guidance in navigating university policies, coordinating schedules, and ensuring that every procedural detail was handled with care played a crucial role in the smooth progression of my thesis work. I am truly grateful for her patience, efficiency, and willingness to help at every stage of my academic progress.

My deepest appreciation goes to my family and friends, and especially to Eli, for believing in me and standing by me through every high and low of this journey. I am profoundly grateful to my parents and siblings whose sacrifices, strength, and enduring belief in me carried us through the challenges of immigration and the many struggles we overcame together. Their love, patience, and wholehearted support were the foundation that held me up in my most difficult moments and gave me the strength to keep going and reach this milestone. My scholarly progress is grounded in their support.

I am deeply grateful to my friend Dr. Sumita Barahmand for her continuous support, genuine care, and honest guidance, especially during moments when I felt broken, as her encouragement gave me the strength and motivation to keep going. Also, to my sweet friend Leena George who always believed in me and encouraged me through the most challenging situations in my lifetime.

I would also like to sincerely recognize Dr. Rouzbeh Sadrimanesh, Dr. Delaram Bineshmarvasti, and Dr. Kimia Masbough for their friendship, encouragement, support, and shared professional insight throughout this journey. Their love, wholehearted support, patience, and encouragement carried me through the most challenging moments of my life.

I would also like to express my sincere and heartfelt gratitude to Saheb Pashaei, whose constant encouragement and joyful athlete spirit made this journey brighter. His vast scientific knowledge, remarkable discipline, and genuine brilliance have been a constant source of inspiration and support for my wellbeing, and his positivity and encouragement during the most difficult time of my life have meant more to me than words can express.

Throughout the course of this research, my home country of Iran has faced immense pressure from both internal and external forces, culminating in the devastating conflict unfolding today. These years have been profoundly difficult, and I hold my country in my thoughts and prayers hoping for peace, resilience, and ultimately freedom.

Chapter 1: History of the Use of Dental Composites

Background

Dental tooth color restorative materials have progressed from early silicate and acrylic systems to modern resin-based composites (RBCs) engineered to emulate tooth structure in function and appearance. RBCs provided a pivotal shift away from amalgam by combining esthetics with improved adhesion and mechanical behavior, yet each advance has necessarily balanced durability, esthetics, handling, cost, and biocompatibility, solving some problems while introducing new constraints (Ferracane et al., 2024; Cramer et al., 2011; Randall & Wilson, 1999).

A landmark in this evolution was the work of Dr. Rafael Bowen at the National Bureau of Standards (now NIST) in the 1960s. The synthesis of bisphenol A–glycidyl methacrylate (Bis-GMA) reduced polymerization shrinkage relative to earlier acrylics and enabled development of composites with superior strength and handling. By incorporating silanized quartz fillers into the Bis-GMA matrix, Bowen established the enduring composite architecture: a polymerizable resin matrix reinforced by inorganic fillers chemically coupled via silane principles that continue to define contemporary RBCs (Ferracane et al., 2024; Wang et al., 2018).

Despite these advances, polymerization shrinkage and the associated interfacial stress remain central challenges, especially in deep cavity preparations and high configuration factor (C-factor) cavities where stress dissipation is limited. Consequences include marginal gaps, postoperative sensitivity, and secondary caries (de Toubes et al., 2022). To mitigate these effects without compromising conversion, modified curing protocols such as soft-start and pulse-delay have been explored, and bulk-fill materials with enhanced photo initiators and polymerization modulators

now permit layering of composites in 4–5 mm increments with moderated stress and improved clinical efficiency (Aguiar et al., 2002; de Menezes et al., 2024).

Concurrently, the emergence of fiber-reinforced composites (FRCs) embedding high-strength fibers within the resin has offered targeted reinforcement for high-load scenarios (e.g., posterior restorations, core build-ups). FRCs improve stress transfer, stiffness, and fracture toughness, and can act as 'stress breakers' that help attenuate polymerization shrinkage–related interfacial strain, positioning them as a strategic complement to advances in curing and material chemistry (Keulemans et al., 2017; Sadr et al., 2020).

Polymerization Shrinkage: An Essential Challenge

Polymerization converts monomer to a crosslinked network, replacing van der Waals interactions with covalent bonds and producing volumetric shrinkage of roughly 2–5% for common methacrylate systems. Shrinkage begins before gelation; after gel point, the material rapidly gains rigidity and transfers stress to the surrounding tooth structure (Ferracane et al., 2024).

The magnitude of shrinkage and stress depends on monomer type and molecular weight (fewer reactive sites per unit volume yield lower shrinkage), degree of conversion, and filler loading (higher filler reduces the shrinking resin fraction). However, clinical impact is governed more by stress development than by volumetric change alone and is modulated by viscoelastic relaxation, cavity geometry (C-factor), and the compliance of surrounding tissues (Cramer et al., 2011; Wang et al., 2018; Davidson et al., 1986).

The C-factor refers to the ratio between the bonded surface area and the unbonded or free surface area of a cavity. As the C-factor becomes higher, the resin composite tends to show reduced

bonding quality and diminished adaptation to the cavity walls. (Yoshikawa et al. 2022). High C-factor preparations (e.g., Class I) restrict flow and amplify stress for a given volumetric change, increasing risk to marginal integrity (Panitvisai & Messer, 1995). Accordingly, research has focused on extending the pre-gel phase to permit stress relaxation (e.g., soft-start/pulse-delay protocols), developing lower-shrink monomers, and incorporating stress-relieving additives. While progress is notable, polymerization shrinkage remains an essential challenge that continues to drive innovation in restorative materials and techniques (Dietrich et al., 1999; Aguiar et al., 2002; de Menezes et al., 2024).

Fiber Reinforcement Overview

Fiber-reinforced composites (FRCs) extend the capabilities of particulate-filled RBCs by embedding continuous or short fibers that preferentially carry load. Efficient stress transfer from the more compliant resin to stiff fibers increases stiffness, toughness, and load-bearing capacity. Because fibers are anisotropic, reinforcement can be oriented along principal stress trajectories to support specific structures in high-load environments such as extensive posterior restorations, indirect restorations, and endodontic core build-ups (Keulemans et al., 2017).

Beyond strengthening, FRCs can moderate polymerization-shrinkage effects (Sadr. et.al., 2020). Strategic placement of a fiber layer at the cavity floor or ‘wallpapered’ along cavity walls absorbs and redistributes curing stress, reducing gap formation compared with incremental or bulk-fill approaches. Contemporary techniques typically confine fibers internally beneath a conventional composite overlay to preserve polishability and esthetics, addressing limitations of earlier exposed-fiber restorations (Keulemans et al., 2017; Ganesh & Tandon, 2006).

Reinforcement efficacy depends on fiber–matrix coupling, adequate critical fiber length, orientation, and architecture. Silanization enhances bonding for glass fibers, whereas plasma or other surface activation improves adhesion to polyethylene fibers. Toughening mechanisms such as crack deflection, bridging, and fiber pull-out increase energy dissipation and contribute to restoration longevity (Keulemans et al., 2017; Sadr et al., 2020).

A spectrum of fiber systems is available, each with distinct handling, esthetic, and mechanical profiles.

- E-glass: Widely used due to balanced strength, translucency, and silane-mediated chemical compatibility with dental resins; suitable for posts, bridges, and direct restorations (Keulemans et al., 2017).
- Ultra-high molecular weight polyethylene (UHMWPE): Very high tensile strength and impact resistance with low density; requires surface activation (e.g., plasma treatment) to enhance bonding; exemplified by leno-weave fiber for splinting and reinforcement (Ganesh & Tandon, 2006; Sadr et al., 2020).
- Carbon/graphite: High strength and stiffness but limited esthetically by dark color; useful for substructures or non-visible applications (Keulemans et al., 2017).
- Aramid (e.g., Kevlar): High tensile strength and abrasion resistance but challenging handling, poor compressive properties, and yellow coloration restrict indications (Keulemans et al., 2017).
- Natural fibers (silk, cellulose): Biocompatible and sustainable but largely experimental in dentistry due to variability and sourcing challenges (Keulemans et al., 2017; Sadr et al., 2020).

These materials support a breadth of indications from direct FRC restorations and conservative fixed dental prostheses to endodontic posts, periodontal splinting, and orthodontic retention where structural preservation is paramount. In endodontically treated teeth with extensive loss, fiber-reinforced strategies offer minimally invasive reinforcement that conserves remaining tooth structure while providing load-bearing support (Deliperi, 2008; Soares et al., 2016; Ganesh & Tandon, 2006) .

Outcomes remain technique-sensitive, hinging on correct fiber selection, architecture, surface treatment, and placement. Esthetic constraints of darker fibers and the persistent role of metal–ceramic frameworks in extreme load cases underscore the need for standardization and robust long-term clinical data to refine indications and protocols (Keulemans et al., 2017; Sadr et al., 2020). Looking ahead, integrating advanced fiber architectures with bioactive, self-healing, or stress-modulating resin chemistries may further shift the paradigm from passive restoration to active preservation. This trajectory from Bowen's Bis-GMA composites to contemporary FRCs highlights the value of sustained collaboration among polymer chemists, materials scientists, engineers, and clinicians in advancing restorative dentistry (Alleman & Deliperi, 2013; Sadr et al., 2020).

A recent systematic review investigated 23 in vitro and 5 clinical studies on short FRC. In vitro studies consistently showed that restorations incorporating short FRCs achieved higher fracture resistance and a greater proportion of repairable failures compared with conventional composites, particularly in large MOD cavities and endodontically treated teeth. Clinical studies, with follow-up periods of up to 4 years, confirmed favorable survival rates and satisfactory marginal adaptation, although no clear superiority over conventional composites was demonstrated (Fernández et al., 2026).

This thesis will include two main experiments on characterization of continuous and short fiber reinforced dental composites using optical coherence tomography and mechanical testing by the 3-point bending test. Chapter 2 focuses on shrinkage related gaps in short fiber and conventional bulk fill composites, with and without continuous fiber reinforcement. Chapter 3 investigates the flexural strength and stress-strain behavior of short fiber and conventional bulk fill composites,

with and without continuous fiber reinforcement, and chapter 4 focuses on discussions and future directions.

Figures

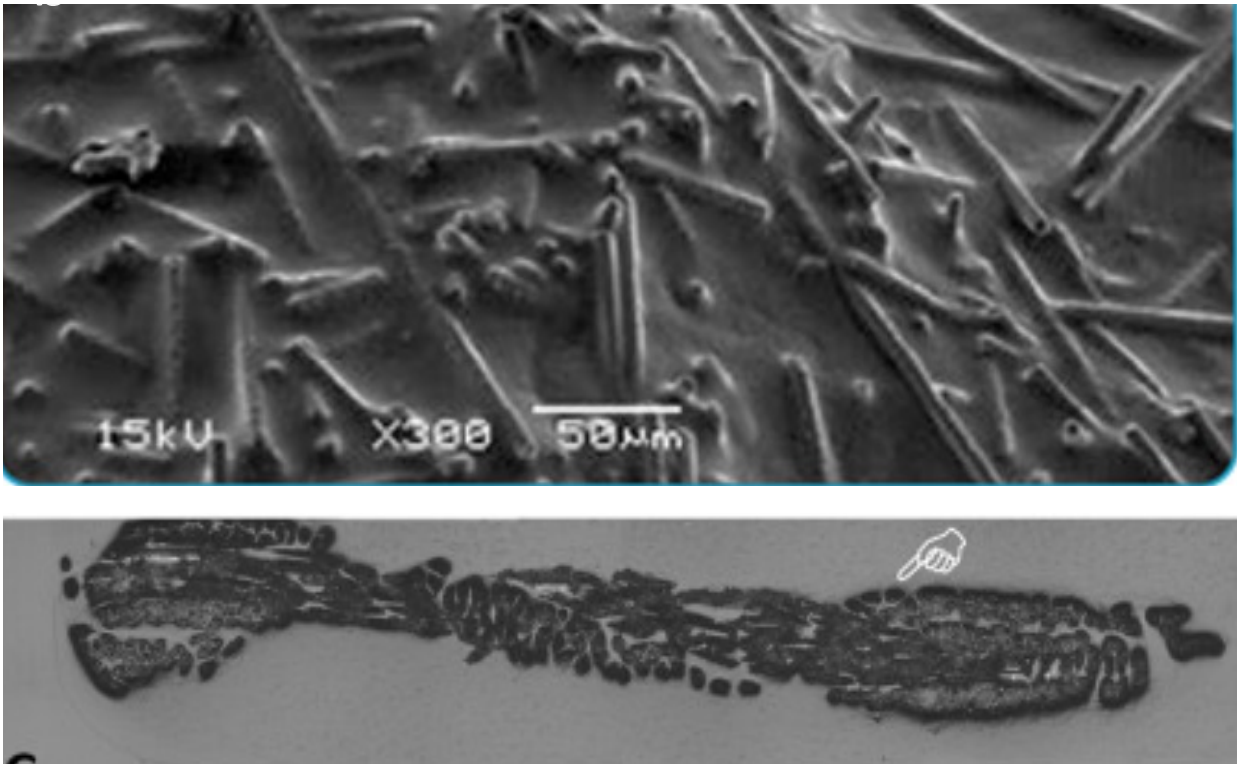

Figure 1. Top: Scanning electron microscope (SEM) image of a short E-glass fiber composite within a resin matrix; Bottom: Confocal laser scanning microscope image of UHMWPE fiber incorporated into a particulate flowable composite. Adapted from Sadr et al. (2020).

Chapter 2: Optical Coherence Tomography; Shrinkage and Gaps Study

Abstract

Background: Polymerization shrinkage of resin composites remains a major limitation in direct restorative dentistry, often leading to interfacial stress, debonding, and gap formation in deep, high C-factor cavities. These shrinkage-related defects can compromise marginal integrity and long-term clinical success. Optical Coherence Tomography (OCT), a noninvasive imaging modality capable of detecting microscale discontinuities, provides real-time visualization of internal gap formation during curing. This study aimed to compare the shrinkage behavior and interfacial adaptation of short-fiber-reinforced composites and bulk fill materials, with and without a continuous ultra-high molecular weight polyethylene (UHMWPE) fiber layer (Ribbond), to determine whether fiber reinforcement improves adaptation at the cavity floor.

Methods: Standardized cubical Class I–type cavities Class I–type cubic cavities (4 mm × 4 mm × 4 mm) were prepared in resin molds and restored with either of three composites material (everX Flow, everX Posterior, or SDR Flow). Each material was tested with and without the incorporation of a continuous Ribbond reinforcement at the cavity floor. Swept-source OCT imaging was performed throughout placement and polymerization to record shrinkage-related separation in real time. Three-dimensional OCT datasets were exported into Amira software, where segmentation of the adhesive interface enabled calculation of the sealing floor area percentage (SFA%) representing gap-affected regions. Volumetric shrinkage (VS%) was also quantified for bonded and, when applicable, unbonded tube specimens. A minimum of ten samples per group were evaluated.

Results: OCT scans of non-reinforced specimens demonstrated bright, irregular high-backscatter regions corresponding to internal separations and microgaps produced by polymerization shrinkage. Continuous reinforcement significantly reduced gap formation across all materials tested. Gap percentages decreased from approximately 30% to 9–10% in everX Flow, from roughly 21–22% to 17–18% in everX Posterior, and most dramatically from 35–36% to 8–9% in SDR Flow. Reinforced specimens displayed more uniform OCT grayscale images with minimal internal voids, indicating improved stress distribution and preservation of interfacial contact. In reinforced groups, the continuous fiber layer acted as an internal stress-absorbing framework and prevented the formation of major micro gaps at the cavity floor.

Conclusion: Incorporating a continuous fiber layer substantially improved interfacial adaptation and reduced polymerization-induced gap formation in all tested composite systems. The greatest improvement occurred in SDR Flow, a high-shrinkage bulk-fill flowable resin. OCT imaging confirmed that fiber reinforcement minimizes shrinkage stress concentration at the cavity floor and promotes more stable contact between the restorative material and cavity surfaces. These findings support the integration of fiber reinforcement strategies, particularly the continuous fiber as an effective method to enhance the performance of composite restorations in deep, high-stress posterior cavities.

Background and Significance

Resin composites have become widely accepted as dependable restorative materials over the past several decades, however, polymerization shrinkage remains a persistent challenge, particularly in large and deep restorations where bulk-placed composites must maintain intimate adaptation to the cavity floor (Hayashi et al., 2019). As the material shrinks during curing, stresses develop along

the cavity walls, enamel margins, and dentin surfaces, which can lead to interfacial debonding, crack propagation, and structural compromise of the tooth-restoration complex. To mitigate these effects, both continuous and short-fiber reinforced composites have been explored as strategies to improve mechanical performance and reduce the likelihood of crack formation (Sadr et al., 2011). In recent years, Optical Coherence Tomography (OCT) has enabled real-time, noninvasive visualization of gap formation within restorations (Fig. 2). OCT provides high-resolution cross-sectional imaging capable of detecting discontinuities as small as a few micrometers (Shimada et al., 2015; Sadr et al., 2011). This technology offers a unique opportunity to study interfacial behavior during composite polymerization, making it possible to directly compare the performance of continuous and short-fiber reinforced materials against traditional bulk-fill composites.

The reinforcing effect of fiber reinforced composites or FRCs depends on multiple factors, including fiber type, orientation, position within the restoration, volume fraction, and the degree of resin impregnation (Alani & Toh, 1997; Belli et al., 2009). Numerous studies have demonstrated their potential for improving the structural reliability of composite restorations. There is currently limited systematic evidence comparing the combined use of continuous fiber reinforcement with short fiber–reinforced bulk-fill composites. Most previous studies have relied on destructive mechanical testing methods, such as microtensile bond strength, which do not allow visualization of gap formation in real time during polymerization. As a result, the influence of continuous fiber layers on interfacial adaptation, particularly at the cavity floor in deep, high C-factor restorations, remains poorly understood. Despite this, little is known about how continuous chairside-placed fibers such as ultrahigh molecular weight polyethylene (UHMWPE) fibers interact with bulk-fill composite resin in deep cavities. Moreover, to the best of our knowledge, investigation and visualization of gap formation in combination of fiber reinforcements

has not been previously tested and visualized in real time using OCT. This research was designed to address this gap.

OCT, originally developed from low-coherence interferometry and widely used in ophthalmology, has significant potential for dental diagnostics (Gabriele et al., 2011). Its ability to visualize internal structures with micron-level precision allows for detailed assessment of cavity morphology and interfacial adaptation. For example, three-dimensional OCT renderings and corresponding cross-sectional B-scans can clearly illustrate cavity walls, the pulpal floor, and restoration interfaces, enabling accurate quantification of gap formation (Shimada et al., 2015; Sadr et al., 2011)

Because OCT has not yet been widely integrated into clinical dentistry, our research served two important purposes. First, it aimed to clarify the differences between continuous and short fiber-reinforced composites, providing evidence to guide clinical decision-making, particularly in structurally compromised teeth where crack prevention is essential.

Second, it advanced understanding of how fiber reinforcement interacts with composite polymerization in deep cavities. Previous studies evaluating ultra high molecular weight poly ethylene fiber or UHMWPE (Ribbond Ultra, Ribbond Inc., Seattle, WA) at the cavity base found no significant change in microtensile bond strength or gap formation when fibers were incorporated; however, these studies did not examine combinations with bulk fill resins nor employ OCT imaging as a diagnostic tool (Alani & Toh, 1997; Belli et al., 2009). By using OCT to visualize gap formation and interfacial adaptation in real time,

this research aimed to provide new insights into the structural and mechanical behavior of fiber-reinforced composites for direct restorations. This combined perspective highlighted the clinical importance of managing polymerization shrinkage, the potential advantages of fiber reinforcement, and the innovative role of OCT in evaluating restorative outcomes. The

effectiveness of fiber-reinforcement is dependent on many variables, including the resins used, the quantity of fibers in the resin matrix, length of fibers, form of fibers, orientation of fibers, adhesion of fibers to the polymer matrix, and impregnation of fibers with the resin (Vallittu, 1996). Short random fibers provide an isotropic reinforcement effect in multi-directions instead of 1 or 2 directions (Vallittu, 1996).

Optical Coherence Tomography (OCT)

Optical Coherence Tomography (OCT) (Fig. 2) has not yet been adopted as a clinical diagnostic technology in dentistry. One innovative aspect of this research was that it represented, to the best of the researcher's knowledge, the first comparison of continuous and short fiber reinforced composites in direct restorations using state of the art OCT imaging. The OCT system employed in this study was a recently developed research grade device that remained unavailable to dental practitioners, making the resulting data uniquely valuable. This work focused on assessing the diagnostic capabilities of OCT while simultaneously examining the structural and mechanical characteristics of fiber reinforced composites. By providing high resolution visualization of features not detectable through conventional methods, the approach offered new insight into the behavior of these materials within deep restorations. Figure 3 represents three-dimensional OCT rendering and cross-sectional B-scan of the standard wide and deep occlusal preparation in an injection modeled epoxy resin lower first molar, illustrating the uneven pulpal floor with a central deepest point and the high-resolution delineation of cavity walls, floor, and restoration interface for evaluating interfacial gaps. This OCT image was collected at the" Biomimetics Biomaterials Biophotonics and Technology" (B4T) lab at the University of Washington School of Dentistry in 2023. In this study, ImageJ was used to segment the gaps at the interface and to compute the

percentage of the cavity surface that was occupied by gaps, so the different materials and continuous fiber layer (UHMWPE) groups could be compared objectively.

Given the clinical importance of maintaining reliable adaptation in high C-factor cavities, we designed our study to investigate gap formation at the cavity floor in real time with OCT, as described in the following null hypothesis.

In this study, the null hypothesis was that there was no difference in cavity adaptation after light polymerization between bulk-fill resin composites used alone and the same materials used in combination with continuous fiber reinforcement. To investigate that, gap formation at the cavity floor was evaluated in real time using optical coherence tomography (OCT), under the assumption that cavity adaptation would remain unchanged whether the composites were placed as particulate composites alone or reinforced with short and/or continuous fibers.

Materials and Methods

Cubical Class I–type cavities (4 mm × 4 mm × 4 mm) were prepared in standardized resin molds and restored with the designated test materials according to the manufacturers' instructions.

The experimental groups were everX Flow (GC Corporation, Tokyo, Japan), everX Flow with Ribbond reinforcement (Ribbond Inc., Seattle, WA, USA), everX Posterior (GC Corporation, Tokyo, Japan), everX Posterior with Ribbond, SDR Flow (Dentsply Sirona, Charlotte, NC, USA), and SDR Flow with Ribbond.

Optical Coherence Tomography Experiment

In this thesis, a prototype OCT system (Yoshida Dental OCT, Yoshida Mfg., Tokyo, Japan) with 12.13 mW output power, a center wavelength of 1310 nm (bandwidth 140 nm), and a 50-kHz sweep rate was utilized. The optical resolution of the system transversely was 40 μm, and the depth resolution was 11 μm in air (translating to 7–8 μm in tissues with a refractive index of around 1.5).

During polymerization of the resin composites, the OCT probe was placed beneath the mold specimen so that the formation of the internal defect at deeper regions of the restoration adjacent to the cavity floor could be imaged through the 0.5-mm-thick mold. The XZ cross-sectional views (B-scans) at the center of the mold and en-face views were recorded continuously in real time as a Windows Media (Yoshida Dental Mfg. Co., Tokyo, Japan) video file at a resolution of 800 × 600 pixels and 20 frames per second. Three-dimensional scans were obtained immediately after light-curing at 400 × 400 × 1024 pixels over an XYZ volume of 6 × 6 × 8 mm^3. Immediately after the scanning, OCT was applied from the top of the cavities so that the integrity at the middle and top regions of the restorations in all specimens could be confirmed.

An identical OCT imaging and analysis protocol was applied across all groups. For each specimen, the three-dimensional OCT datasets were segmented at the adhesive interface and the percentage of gap-affected floor area was calculated. Gap formation in deep cavities across all groups was visualized using OCT. A binary image was created by averaging XY slices over a 1000-μm thick region at the floor using the maximum intensity projection (MIP) function of the prototype OCT Viewer Software (Yoshida Mfg.). National Institutes of Health (NIH) image analysis software (ImageJ ver 1.53, Bethesda, MD, USA) software was then used to calculate the gap percentage for each specimen and to generate the corresponding gap area mask used to quantify the separated floor surface. Figure 6 illustrates this process by showing a 2-dimensional OCT cross-section of the gap area in the deep cavity, followed by an OCT image that highlights the gap formation within the restoration, and finally the gap area mask produced through ImageJ software to quantify the extent of floor separation in percentage (%).

The data set was analyzed using two-way ANOVA followed by post-hoc analysis with a significance level of 0.05 (n=8).

Results and Discussion

Visual OCT images of representative specimens in each group are presented in Figures 5 to 10. A bar graph summarizing the gap results is presented in Figure 11 with the accompanying table presenting the statistical analysis. Bulk placement of all the tested composite materials without continuous fiber resulted in some degree of separation of the composite from the cavity floor. The highest nominal gaps, up to complete separation (100%) were observed in the SDR Flow group, followed by everX Flow, which were not significantly different ($p > 0.05$).

The null hypothesis was rejected; two-way ANOVA analysis showed that placement of a base increment of each composite incorporated with continuous fiber improved the adaptation to the cavity floor compared to their corresponding bulk (no continuous fiber) groups ($p < 0.05$). One the other hand, there was no significant difference in adaptation to the floor among the three composite groups ($p > 0.05$). In addition, the interaction of the two factors was not significant ($p > 0.05$). Since both the composite type factors and the interactions were not significant, no further pair-wise comparisons were performed

Visual gap analysis suggested that incorporation of continuous fiber (UHMWPE) reduced the percentage of interfacial gaps for all composites (Fig. 11). The everX Flow exhibited the highest mean gap percentage among the fiber-reinforced materials without continuous fiber layer (30%), which decreased to about 10% when continuous fiber layer (UHMWPE) was added. The high viscosity short fiber composite (everX Posterior) showed a smaller but still notable reduction, from roughly 22% without continuous fiber layer to 17% with it. The bulk fill flowable composite (SDR Flow) demonstrated the greatest benefit from reinforcement, with gap percentage dropping from approximately 35% in the non-reinforced group to around 8% in the continuous fiber layer group.

In OCT images, regions of increased optical backscatter appear as brighter zones because more of the incident light is reflected or scattered back to the detector. Consequently, the bright, irregularly shaped white bands within the composite correspond to areas of increased backscatter that represent internal separation and micro gaps created by volumetric shrinkage during curing. When a resin composite undergoes volumetric shrinkage, it can pull away from the cavity walls or internal structures, forming tiny gaps or separations filled with air or lower density material. These discontinuities have a refractive index different from the surrounding composite, so they scatter light strongly and appear as high-intensity (white) areas on the B-scan. Thus, clusters or bands of bright signal within or along the restoration margins are interpreted as internal separation and micro gaps associated with polymerization shrinkage rather than an intact, well-adapted interface. Along the cavity walls and floor these high-intensity zones indicate partial loss of intimate contact between the fiber-reinforced composite and the surrounding substrate, consistent with shrinkage-related debonding in a high C-factor configuration.

Figures 5 and 6 represent the OCT B-scan of the short E-glass fiber-reinforced everX Flow specimen restored with and without an additional continuous fiber layer (UHMWPE) respectively. UHMWPE was placed at the cavity floor. The continuous fiber layer acts as a stress absorbing cushion (Sadr et. al 2020) within the composite. During curing, the composite still shrinks, but part of the stress is taken up and redistributed along the flexible fiber ribbon rather than being concentrated at the cavity walls. This reduces interfacial pulling and separation, so few or no micro gaps form (Sadr et. al 2020). Because those gaps and separations create the bright, high backscatter "white" areas on OCT, their absence yields a more uniform, darker image, with the continuous fiber appearing as the only bright structure. The bright, well defined central band corresponds to the highly scattering UHMWPE ribbon, which presents a homogeneous white band. Unlike the

nonreinforced specimen, there are no discrete bright gaps or separation lines along the cavity walls and floor, indicating that volumetric shrinkage during polymerization did not produce detectable interfacial debonding in this configuration. Collectively, these images indicate that the continuous fiber layer acted as a stress absorbing intermediate, redistributing polymerization shrinkage stresses and thereby minimizing or eliminating shrinkage related separation at the adhesive interface.

Figures 7 and 8 represents an SDR Flow specimen restored with and without UHMWPE reinforcement. SDR Flow is a radiopaque bulk fill flowable resin composite that does not contain reinforcing fibers; thus, polymerization shrinkage stresses are borne by the resin matrix and its bond to the cavity walls. The bright vertical streaks and localized white zones in figure 9, (no-UHMWPE) extending from the occlusal surface toward the cavity floor represent increased optical backscatter, consistent with micro gaps likely formed as the material shrank away from the surrounding structure during curing. These discontinuities indicate less favorable adaptation of the non-fiber reinforced bulk fill composite in deep, high C-factor preparations compared with configurations that include an intermediate fiber layer. By acting as an internal stress absorbing framework, the UHMWPE fiber reduced debonding at the interfaces, so far fewer micro gaps formed between the composite and the surrounding structure. As a result, the high intensity white bands that previously indicated voids or internal separation are markedly diminished, and the composite bulk appears more uniformly gray, consistent with improved adaptation and reduced gap formation after curing.

Figures 9 and 10 present the everX Posterior restoration, with-out and with UHMWPE respectively. The material used was everX Posterior which is a short E-glass fiber reinforced composite used as a dentin replacement substructure. It is important to mention that this material is now discontinued. Despite the internal reinforcing fibers, the bright vertical white

lines and streaks within the composite indicate areas of increased optical backscatter that correspond to internal separation or voids formed as the material shrank during polymerization. These high intensity bands represent micro gaps along the cavity walls or within the bulk of the restoration where the composite has partially pulled away, reflecting residual polymerization shrinkage stresses even in this fiber reinforced material.

In figure 10, the everX Posterior restoration with UHMWPE shows a continuous, uniform interface without bright, high backscatter bands that would indicate true internal separation or marginal gaps. The vertical white lines visible within the composite are imaging artifacts produced when the specimen's outer surface was smoothed with a polisher, not defects created by polymerization which is easily identified by the observation of specimen and the outer location of the lines even in the areas that composite does not exist. When UHMWPE was used, because the continuous fiber layer acts as an internal stress absorbing framework, it redistributed and reduced polymerization shrinkage stresses, so the composite did not pull away from the cavity walls or from the underlying structure. As a result, shrinkage-related micro gaps were minimized, and the restoration appears well adapted throughout its depth, confirming that the UHMWPE reinforcement effectively reduced shrinkage induced gap formation in this specimen.

Conclusion and Clinical Relevance

Collectively, these findings indicate that the incorporation of a continuous fiber layer substantially improved interfacial adaptation and minimized shrinkage-related gap formation, particularly in the high-shrinkage bulk-fill flowable composite, but still benefitted the short fiber composites, particularly the low viscosity type.

Building on these results, future research should investigate optimal fiber placement strategies (e.g., thickness, position, and orientation at the cavity floor), evaluate different fiber chemistries and

bonding protocols, and validate performance under thermomechanical aging and cyclic loading to better simulate intraoral conditions. Larger in vitro datasets and well-designed randomized clinical trials are also warranted to determine longevity, failure modes, and cost-effectiveness across diverse cavity geometries and C-factor scenarios.

From a clinical standpoint, the use of a chairside continuous fiber layer (e.g., UHMWPE ribbon) may offer a practical method to redistribute polymerization stresses, preserve adhesive contact at the pulpal floor, and reduce the risk of marginal leakage and postoperative sensitivity in deep posterior restorations. In cases restored with bulk-fill flowable composites, where shrinkage stresses are more pronounced, this approach could improve restoration durability, decrease the incidence of repair or replacement, and enhance overall treatment predictability.

Figures and Tables

Figure 2. Optical coherence tomography (OCT) imaging setup used to capture cross-sectional images of samples in the University of Washington laboratory.

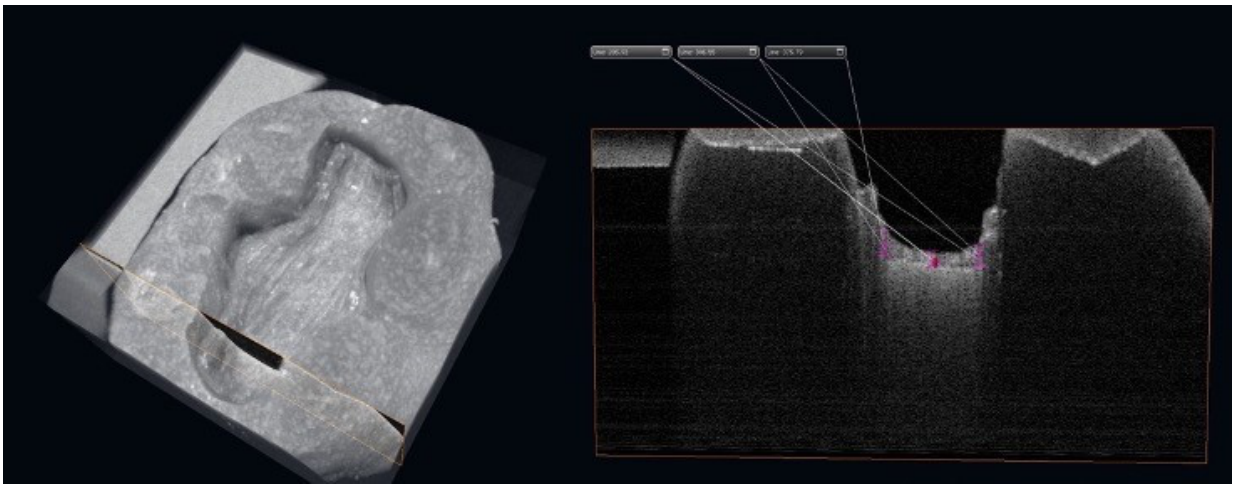

Figure 3. Three-dimensional OCT rendering (Amira) and cross-sectional B-scan of the standard wide and deep occlusal preparation in an injection modeled epoxy resin lower first molar, illustrating the uneven pulpal floor with a central deepest point and the high resolution delineation of cavity walls, floor, and restoration interface for evaluating interfacial gaps.

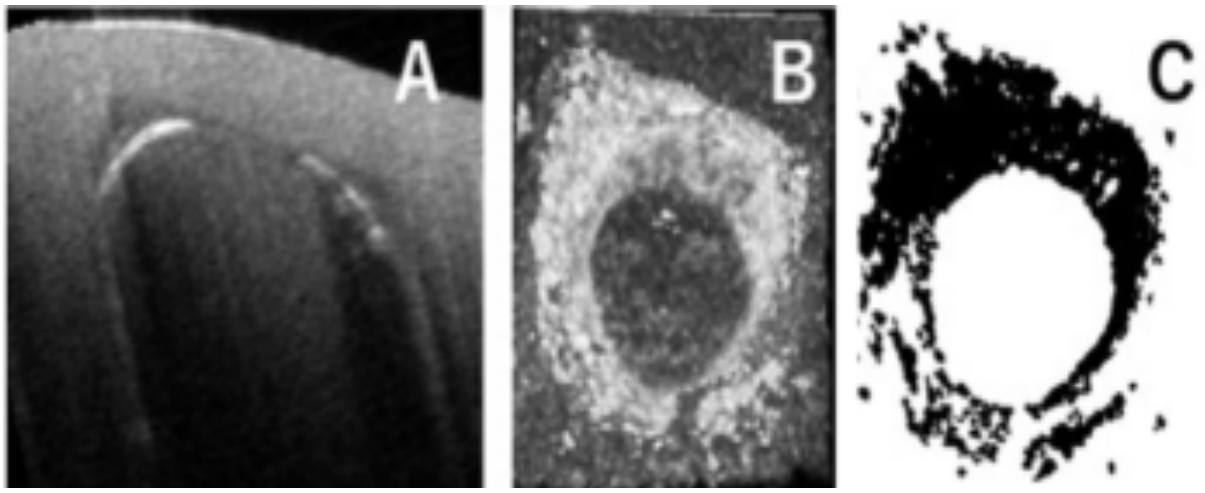

Figure 4. Gap formation in a deep cavity representing SDR flow bulk field. A) 2D OCT image cross section of gap area in the deep cavity. B) OCT image of ap formation in the deep cavity. C) Gap area mask measurement using ImageJ software

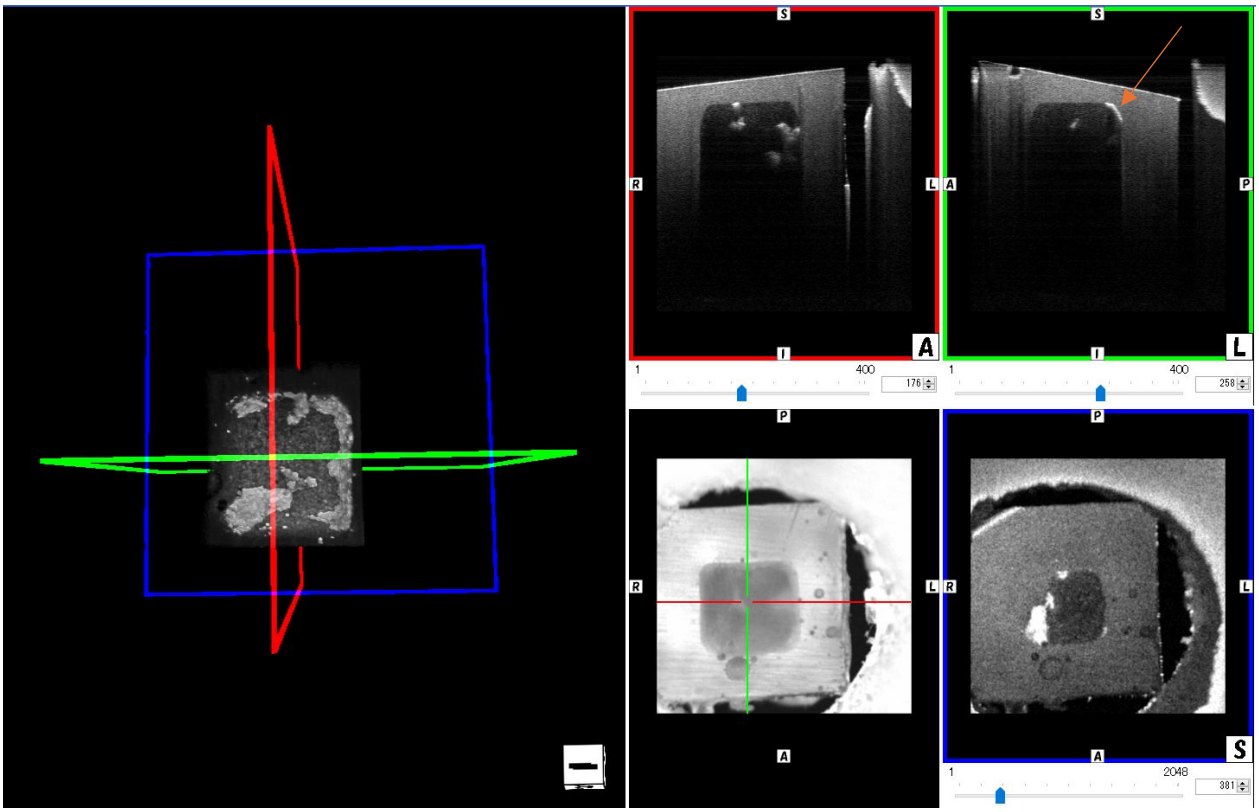

Figure 5. OCT screenshot of specimen restored with short Eglass fiber-reinforced everX Flow without continuous fiber reinforcement imaged after polymerization. The left side panel presents a 3D reconstruction of the scan, which was later subjected to binarization and gap area calculation. White scattered lines present gap formation.

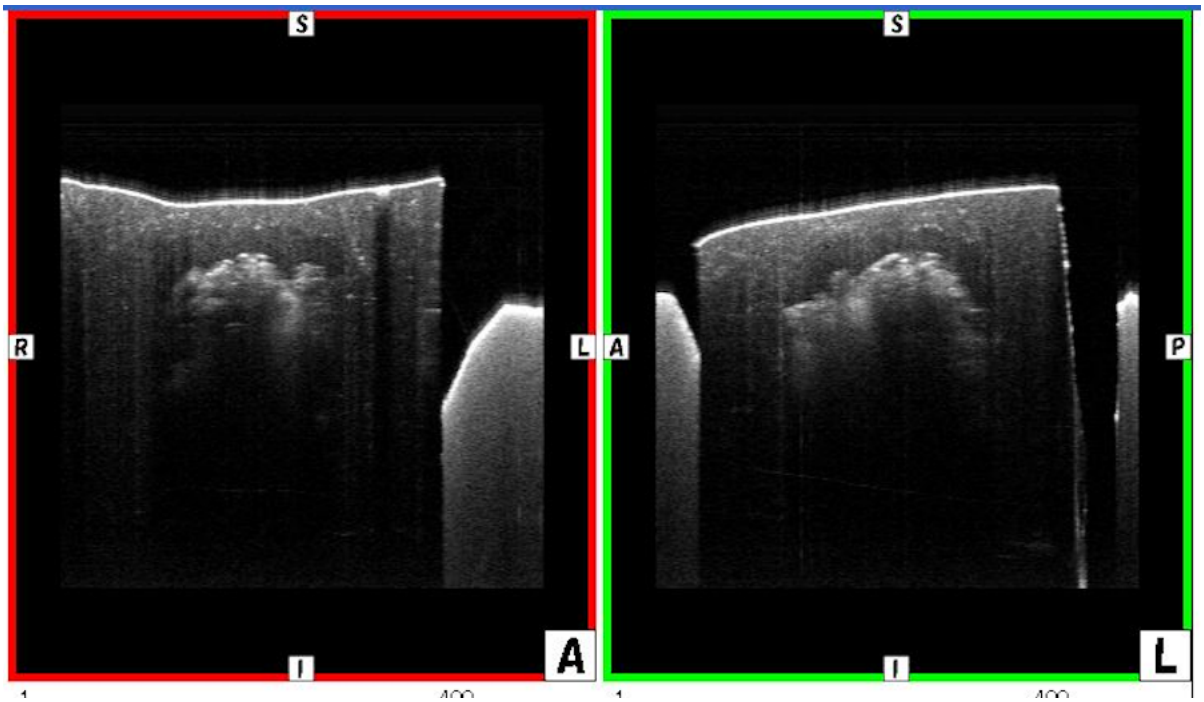

Figure 6. OCT scan that illustrates a short Eglass fiber reinforced (everX Flow) specimen with continuous fiber reinforcement imaged in cross-section after polymerization.

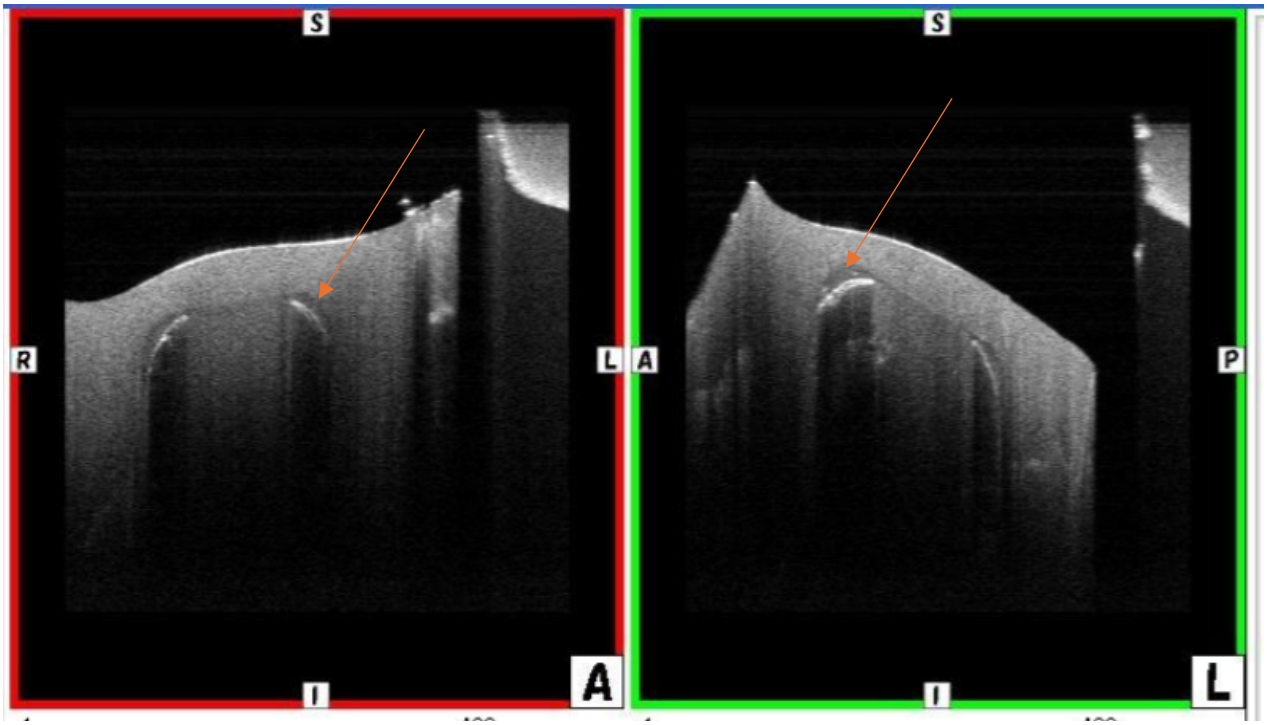

Figure 7. OCT scan illustrating an SDR Flow bulk fill flowable composite specimen without fiber reinforcement, imaged in cross-section after polymerization. White scattered lines present gap formation.

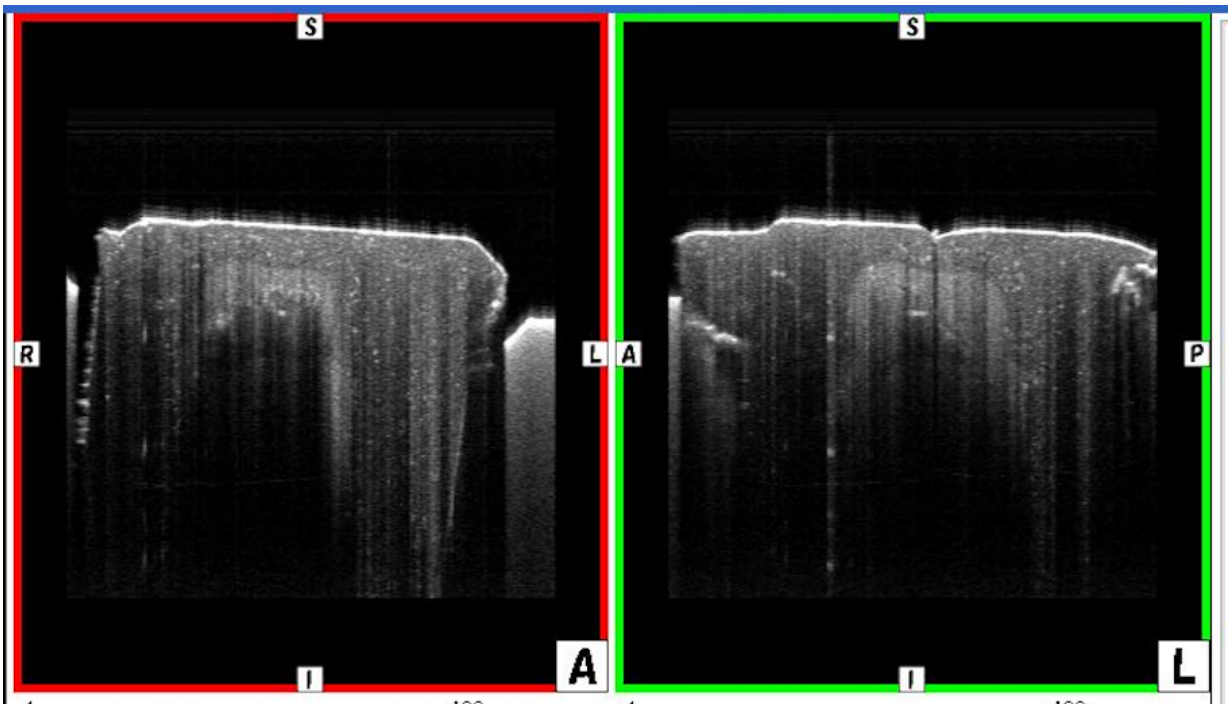

Figure 8. OCT scan illustrating an SDR Flow bulk fill flowable composite specimen with continuous fiber reinforcemen, imaged in cross-section after polymerization.

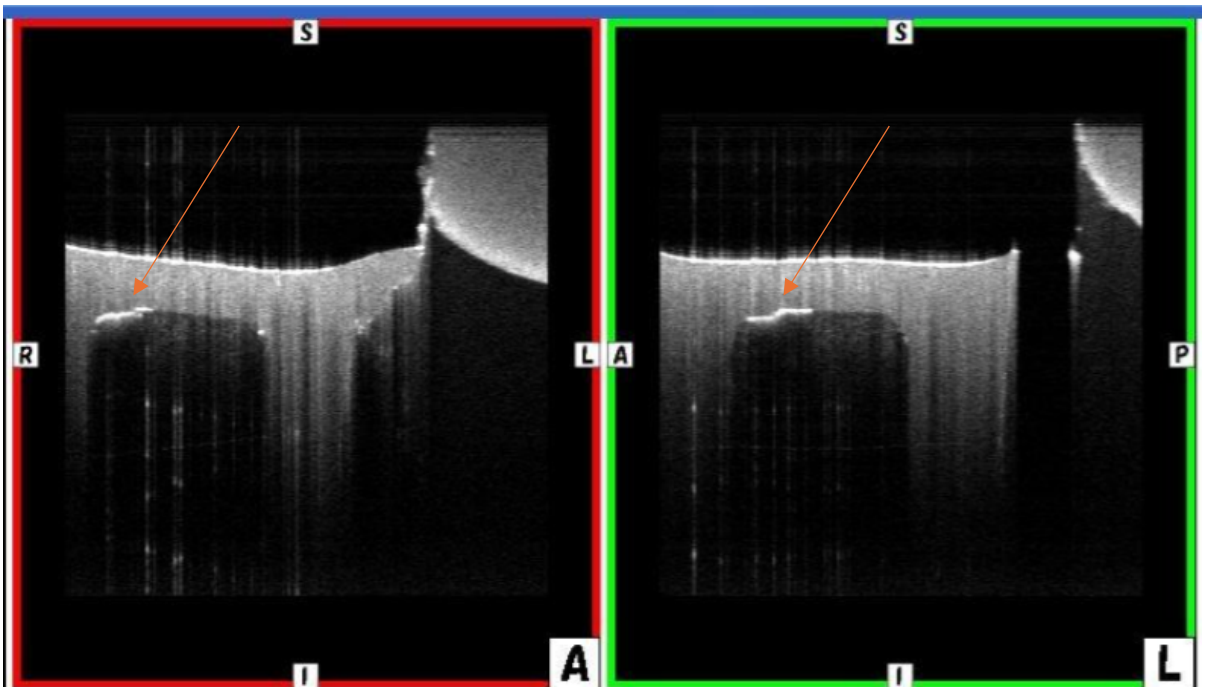

Figure 9. OCT scan illustrating an everX Posterior composite specimen with no extra fiber reinforcement (Ribbond), imaged in cross-section after polymerization. White scattered lines present gap formation.

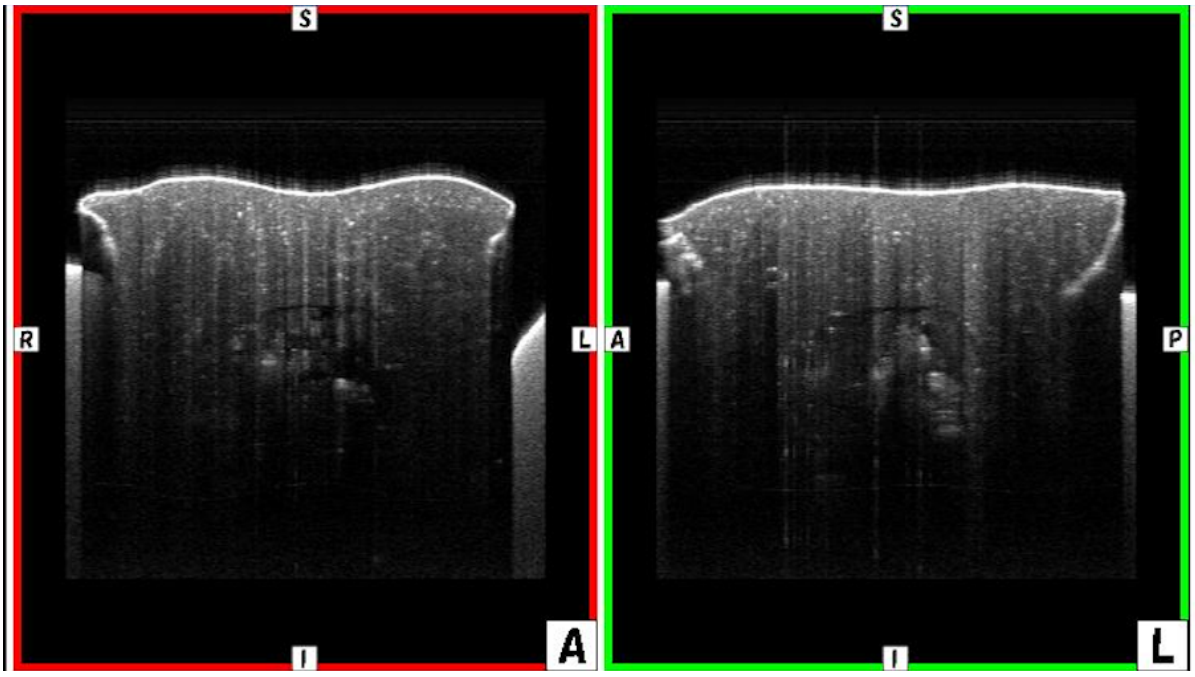

Figure 10. OCT scan illustrating an everX Posterior composite specimen with fiber reinforcement (Ribbond), imaged in cross-section after polymerization.

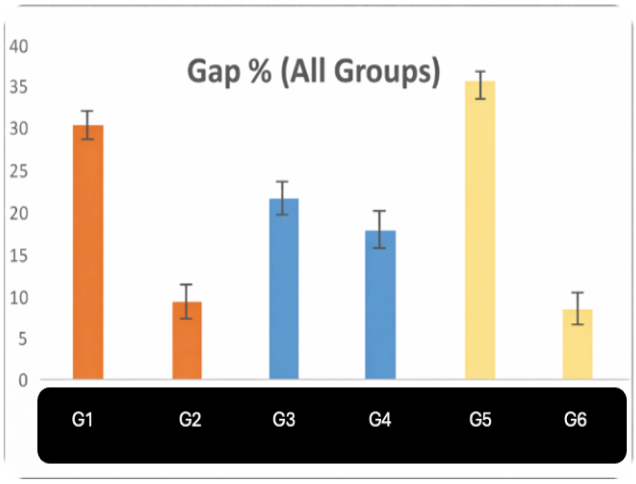

Gap percentage for all composite groups

Group	Description
G1	Short fiber (everX Flow)
G2	Short + continuous fiber (everX Flow + Ribbond)
G3	Short fiber (everX Posterior)
G4	Short + continuous fiber (everX Posterior + Ribbond)
G5	Bulk-fill composite (SDR Flow)
G6	Bulk-fill + continuous fiber (SDR Flow + Ribbond)

Figure 11. Gap percentage for all composite groups, showing marked reduction in gap formation when Ribbond reinforcement was incorporated into everX Flow, everX Posterior, and SDR Flow restorations.

Factor	F	p
Continuous Fiber	5.79	**0.024***
Composite Type	0.34	0.72
Interaction	0.87	0.43

Table – Two-way ANOVA results for the OCT Gap Percentage.

* p value is significant for the factorial analysis at 0.05 level.

Chapter 3: Flexural Strength

Abstract

Background: Flexural strength is a key mechanical property of dental composites, reflecting their ability to withstand tensile and compressive stresses in the oral environment. Fiber reinforced composites (FRCs) have been developed to overcome the limitations of conventional particulate filled materials by improving stress transfer, crack deflection, and fracture resistance. This study evaluated the effect of polyethylene fiber reinforcement on the flexural strength and failure behavior of several direct restorative composites.

Methods: Composite bars were fabricated according to ASTM D7264/D7264M06 using a silicone mold. Four composites everX Flow, SDR Flow+, GrandioSO, and Filtek Universal were tested with and without continuous fiber reinforcement. For reinforced groups, Ribbond fibers were prewetted with CLEARFIL SE Bond 2 and embedded in the lower third of the specimen. All specimens were lightcured per manufacturer instructions. Flexural strength was measured using a threepoint bending test on an Instron Electro Puls E1000 machine at 0.5 mm/min with a 26 mm support span. Eight specimens per group were tested, and data were analyzed using twoway ANOVA (Fig. 13).

Results: Continuous fiber reinforcement increased mean flexural strength across all composite types. Two-way ANOVA showed significant effects of composite type ($F(3,48) = 11.06$, $p < 0.001$) and continuous fiber application ($F(1,48) = 5.40$, $p = 0.024$), with no significant interaction, indicating a consistent reinforcing effect. The short fiber reinforced composite (everX Flow) exhibited significantly higher flexural strength than regular composites (Filtek, GrandioSO, and SDR Flow) . The failure mode differed prominently: non-reinforced specimens fractured abruptly

into separate pieces, while continuous fiber-reinforced specimens showed more ductile behavior, remaining intact or only partially separated due to fiber bridging.

Conclusion: Polyethylene fiber reinforcement enhances both flexural strength and fracture resistance of all tested resinbased composites. The shift from brittle, catastrophic failure to more controlled, cohesive fracture patterns demonstrate improved energy absorption and crack bridging behavior. These findings support the use of fiber reinforcement particularly Ribbond as an effective strategy to improve the mechanical performance and durability of direct composite restorations, especially in high stress clinical situations.

The Significance of Flexural Strength

As the use of dental composites has expanded, flexural strength has become an important predictor of clinical performance and durability (Cramer et al., 2011). Flexural strength is a key mechanical property of dental restorative materials because it reflects a material's ability to withstand functional stresses in the oral environment. Because composites are exposed to occlusal loading, thermal cycling, and chemical challenges, flexural strength testing provides a useful basis for predicting restoration performance and guiding material selection (Drummond et al., 2009). Clinically, materials with higher flexural strength generally show better marginal integrity, lower wear, greater longevity in high-stress areas, and improved resistance to long-term cyclic deformation (Heintze et al., 2010; Coldebella et al., 2009).

Role of Fillers in Flexural Strength

The flexural strength of dental composites is closely related to their composition, including both the inorganic filler phase and the organic resin matrix. A strong positive relationship has been reported between filler weight percentage and flexural strength, as higher filler loading improves stress transfer and limits polymer chain mobility under load (Mata et al., 2011). Filler size, morphology, and distribution are also important; for example, microhybrid composites generally exhibit higher flexural strength than micro filled materials because of their more favorable filler distribution (Masouras et al., 2008). A study done by Dr. Chung and his research group on the flexural strength of resin-based materials found that orienting fibers horizontally on the tension side of the specimens produced a statistically significant increase in flexural strength compared with the control group. In the same study, it was concluded that the inclusion of glass fibers enhanced the flexural strength of the resin, with the dispersed-fiber method proving more effective than

the oriented-fiber approach. Another study indicated that the filler–resin interface, strengthened by silane coupling agents, is critical because weak bonding can create sites for crack initiation and propagation (Van Noort et al., 2007). The resin matrix also contributes significantly, as crosslink density, degree of conversion, and overall polymer network properties influence resistance to deformation (Calheiros et al., 2013).

Evolution of Fiber-Reinforced Composites

Fiber-reinforced composites (FRCs) represent an important advance in dental materials by addressing many of the mechanical limitations of conventional particulate-filled composites. Glass, polyethylene, and carbon fibers improve performance through stress transfer, crack deflection, and crack-bridging mechanisms, allowing resin-based materials to be used in higher-stress applications that were once dominated by metal-based restorations (Garoushi et al., 2012).

Early generations of dental FRCs introduced randomly-oriented short fibers into traditional composite formulations, but their performance was limited by poor fiber–matrix adhesion, handling, and surface finish (Garoushi et al., 2008). Later improvements in fiber surface treatment, especially silanization of glass fibers, greatly enhanced interfacial bonding and reinforcement. Current dental FRCs may contain continuous unidirectional fibers, woven fiber networks, or short randomly oriented fibers, each with distinct clinical advantages. Unidirectional fibers provide maximum reinforcement along the fiber axis while woven fibers offer more isotropic reinforcement, and short random fibers provide intermediate omnidirectional reinforcement with improved chairside handling (Garoushi et al., 2012).

Factors Influencing Flexural Reinforcement in Fiber-Reinforced Composites

Accurate measurement of flexural strength depends on proper specimen preparation, storage, and testing conditions. Fabrication errors such as internal defects, incomplete curing, or dimensional inaccuracies can significantly alter results (Drummond et al., 2009). Standardized preparation typically requires careful placement of material into molds, adequate light curing, and polishing to remove surface irregularities that may act as stress concentrators.

Storage conditions also influence measured values. Water storage has been shown to reduce composite flexural strength by 10%–30% compared with dry storage (Abdul-Monem et al., 2016), and thermocycling can further reduce strength through hydrolytic degradation and thermally induced stresses (Medina Tirado et al., 2012). Testing variables must also be controlled as loading rate can affect measured strength because of viscoelastic behavior, and proper specimen alignment and machine calibration are essential for repeatable results (Heintze et al., 2010; International Organization for Standardization, 2000).

The reinforcing effect of fibers is mainly due to stress transfer from the weaker resin matrix to the stronger fiber phase, reducing localized stress concentrations and delaying failure (Suzuki et al., 2011). The high tensile strength of fibers, especially glass and carbon fibers, also directly improves resistance to tensile stresses during bending. In addition, fibers enhance toughness through crack deflection and crack bridging. When cracks encounter fibers, propagation is redirected or slowed, increasing the energy required for catastrophic failure (Garoushi et al., 2012). The magnitude of reinforcement depends on fiber type, orientation, volume fraction, and interfacial adhesion. Fibers aligned with tensile stress provide the greatest reinforcement, whereas perpendicular fibers are less effective. Higher fiber volume fractions generally improve strength until resin wetting becomes inadequate, making strong fiber–matrix bonding essential (Garoushi et al., 2008).

Comparative Flexural Strength of Fiber Reinforced Composites

Fiber-reinforced dental composites consistently demonstrate higher flexural strength than conventional particulate-filled materials (Garoushi et al., 2012). Comparative studies have reported strength increases ranging from 25% to more than 200%, depending on fiber type, orientation, and testing conditions (Garoushi et al., 2012). This improvement has expanded the use of resin-based restoratives in large posterior restorations, endodontically treated teeth, and temporary fixed dental prostheses.

Among reinforcing fibers, glass fibers, particularly E-glass and S-glass, are widely used because they provide a favorable balance of mechanical properties, esthetics, and cost. Glass fiber-reinforced composites typically show flexural strength values of 160–300 MPa, compared with 80–140 MPa for conventional composites (Garoushi et al., 2008). Polyethylene fibers are also widely used and offer advantages in esthetics and handling. Although their absolute flexural strength is generally lower than that of glass fiber systems, they often provide greater toughness and impact resistance because of their flexibility (Suzuki et al., 2011). This makes them particularly useful in restorations exposed to dynamic loading, such as trauma splints and pediatric applications.

The fiber–resin interface is crucial for effective stress transfer and prevention of premature fiber pullout. Silanated glass fibers form strong chemical bonds, whereas polyethylene fibers require plasma or similar treatment, as demonstrated in the Ribbond system. Fibers also improve fracture toughness by slowing crack propagation under cyclic loading and may enhance restoration longevity. Beyond strengthening, fiber layers can influence polymerization shrinkage stress. Sadr et al. reported in 2020 that placement of a polyethylene fiber layer (Ribbond Ultra) at the cavity floor reduced gap formation in bulk-fill restorations, likely through elastic stress absorption, shrinkage vector redirection, and viscoelastic effects during curing. Similarly in 2017, Deliperi and their research group described the “wallpapering” technique, in which bonded fibers are placed

along cavity walls to optimize reinforcement in structurally compromised teeth. Clinically, FRCs can serve as dentin-replacing materials in large posterior and endodontically treated teeth, reduce shrinkage-related stress, and support fiber-reinforced fixed dental prostheses as esthetic, metal-free alternatives to metal-ceramic bridges.

Short, randomly oriented fiber composites represent another important development because they retain the reinforcing benefits of fibers while avoiding some of the handling limitations of continuous fiber systems. These materials, typically containing 5%–15% by weight of 1–3 mm fibers, have shown flexural strength values 30%–80% higher than conventional composites while maintaining similar clinical handling properties (Garoushi et al., 2012). As a result, they are increasingly used in direct posterior restorations.

Significance: One innovative aspect of this research is that, to the best of the researcher's knowledge, it represents the first investigation comparing the flexural strength of combinations of continuous and short fiber-reinforced composites in direct restorations.

This study compared the flexural strength of direct restorative composites used alone and in combination with continuous fiber reinforcement. The null hypothesis was that there would be no difference in flexural strength between conventional particulate composites and their corresponding fiber-reinforced configurations.

Materials and Methods

For the flexural strength test, bar shaped composite specimens were fabricated in accordance with ASTM D7264/D7264M06, which specifies specimen geometry and loading conditions for determining flexural stiffness and strength of polymer matrix composites using a three point bending configuration. A custom rectangular mold (32 mm length × 4 mm width × 2 mm thickness) was prepared from addition cured silicone dental putty to standardize specimen dimensions and allow easy removal after curing. The composite bars were light cured directly inside the silicone mold to ensure standardized dimensions and minimize handling defects. The mold was positioned on a flat, reflective surface, and the light curing unit tip was placed in close contact with the top surface, perpendicular to the long axis of the specimens. Each segment of the mold was exposed sequentially with slight overlap to cover the entire bar length, using the exposure time and irradiance recommended by the manufacturer. After curing, the specimens were allowed to remain in the mold for an additional period to complete polymerization before being gently removed and inspected for surface defects or voids.

The uncured composite was placed into each mould cavity in incremental layers and carefully adapted to minimize void or air bubbles. In the groups reinforced with polyethylene fiber (Ribbond), precut UHMWPE strips were first conditioned with a two-step self-etch adhesive (CLEARFIL SE BOND 2, Kuraray Noritake Dental Inc., Tokyo, Japan) used as the bonding agent. Ribbond fibers were prepared according to the clinical technique described by Dr. Grant Chyz for fiber reinforced composite restorations (Chyz, 2010). Precut strips were thoroughly wetted with an unfilled bonding resin until fully saturated, and excess resin was removed with a micro brush to prevent pooling. The saturated fibers were then pressed into a thin layer of uncured composite on

a mixing pad to form a composite impregnated Ribbond strip, which was transferred to the mould and positioned within the lower one third of the specimen thickness, fully embedded in the uncured composite and aligned along the long axis of the bar (Chyz, 2010).

All specimens were light cured using an LED curing unit in accordance with the manufacturers' recommended exposure times, with the light guide maintained in close contact with the mould surface to promote uniform polymerization. Eight specimens were fabricated for each experimental group, are presented in Table 2. Specimens were assigned to eight groups based on composite type and presence or absence of Ribbond reinforcement, as summarized in Table 2.

Flexural Strength Test

In order to test our hypothesis, the three point bending test was chosen for this study, as it is the ISO standardized reference method for dental composites and closely approximates the combined tensile and compressive stresses that restorations experience clinically, enabling meaningful comparison of the flexural performance of different materials. For this study, specimen dimensions were chosen according to ASTM D7264/D7264M06 to allow reliable measurement of flexural properties. The standard support-to-span ratio of 32:1 is recommended by ASTM. A support span-to-thickness ratio of less than 32:1 may be acceptable for obtaining the desired flexural failure mode. Therefore, given the amount of composite required to fabricate these relatively large specimens, the span length to thickness ratio (16:2) and support configuration were selected to comply with the ASTM guideline so that failure would occur at the tensile surface under pure bending during three point loading. For fabric-reinforced textile composite materials, the width of the specimen should accommodate the width of the textile (fiber in this case); therefore, a Ribbond

Ultra THM (3 mm width) was selected for this experiment. Shear deformations can significantly reduce the apparent modulus of highly orthotropic laminates when they are tested at low support span-to-thickness ratios. For this reason, a higher support span-to-thickness ratio is recommended for flexural modulus determinations in these materials. While laminate stacking sequence is not limited by this test method, significant deviations from a lay-up of nominal balance and symmetry may induce unusual test behaviors and a shift in the neutral axis.

We chose our material and groups according to availability, for example everX Posterior was no longer available in the market, therefore was taken out of the studies. The everX Flow (GC, Tokyo, Japan) is a short Eglass fiber reinforced, radiopaque bulk fill flowable composite indicated for dentin replacement and core buildup, as specified in the manufacturer's brochure and safety data sheet. The SDR Flow+ (Dentsply Sirona, Charlotte, NC, USA) is a self levelling bulk fill flowable composite with low polymerization shrinkage stress, intended for posterior restorations and base/liner applications according to the manufacturer's technical description. In this study, both materials were used according to the respective instructions for use, with EverX Flow serving as the short fiber composite and SDR Flow+ as the non-fiber bulk fill control in the OCT and flexural strength experiments. GrandioSO (VOCO, Cuxhaven, Germany) is a universal nano hybrid restorative composite with a high filler content (approximately 89 wt%) intended for anterior and posterior restorations. Filtek Universal Restorative (3M, St. Paul, MN, USA) is a light cured universal nanocomposite indicated for direct anterior and posterior restorations, core build ups, splinting, and indirect inlays/onlays and veneers. Ribbond (Ribbond Inc., Seattle, WA, USA) is a bondable reinforcement ribbon made of ultra high molecular weight polyethylene fibers, designed to be embedded in composite resins for reinforcement in various restorative and splinting applications.

The restorative materials, reinforcing fibers, adhesive system, and curing device used in this study are summarized in Table 1. The tested composites included a short Eglass fiber reinforced bulk fill material (everX Flow) and three non-fiber bulk fill or universal composites (SDR Flow+, GrandioSO, and Filtek Universal Restorative), representing both fiber reinforced and conventional resin based systems. Ribbond ultra high molecular weight polyethylene ribbon was selected as the continuous fiber reinforcement, while CLEARFIL SE Bond 2 served as the wetting resin and a LED curing unit (3M ESPE, St. Paul, MN, USA) was used for photoactivation of all light curable materials according to the manufacturers' instructions.

Flexural testing was performed using a dynamic universal testing machine (Instron Electro Puls E1000, Instron, Norwood, MA, USA) operating in three point bending mode at a crosshead speed of 0.5 mm/min. The Electro Puls E1000 is an electrodynamic testing system that allows precise control of load and displacement and is widely used for characterization of mechanical properties of dental and biomedical materials. A three point bending fixture with a support span of 26 mm was used, and the load was applied at the midpoint between the two supports in a plane perpendicular to the long axis of each specimen. Specimens were loaded until fracture, and the flexural strength was calculated from the maximum load recorded on the machine's load displacement curve.

Results and Discussion

Flexural strength values were obtained using three-point bending testing and calculated in MPa for all experimental groups. Each composite material was evaluated with and without continuous fiber, ultra-high molecular weight polyethylene ribbon fiber reinforcement to assess the effect of fiber incorporation on bending performance.

Across all materials tested, the addition of Ribbond fiber reinforcement resulted in increased mean flexural strength compared to their respective non-reinforced control groups. For everX Flow, specimens reinforced with Ribbond demonstrated higher flexural strength values than the non-reinforced everX Flow group. Similarly, SDR Flow with Ribbond exhibited greater flexural strength compared to SDR Flow without fiber reinforcement. Specimens made with GrandioSO disclosed improved flexural strength following Ribbond incorporation relative to the non-reinforced group. Filtek specimens also demonstrated enhanced flexural strength when reinforced with Ribbond compared to Filtek without fiber.

Overall, the reinforced groups consistently demonstrated superior resistance to bending stress, indicating that incorporation of continuous fiber contributed positively to the flexural performance,

Two-way ANOVA revealed a significant effect of composite type ($F(3,48) = 11.06$, $p < 0.001$) and of continuous fiber application ($F(1,48) = 5.40$, $p = 0.024$). The interaction between composite type and continuous fiber was not statistically significant ($F(3,48) = 1.42$, $p = 0.25$).

Two-way ANOVA (table 3) demonstrated significant main effects of composite type and continuous fiber application. In the post hoc analysis (Tukey), the short fiber reinforced (everX) exhibited significantly higher values compared with regular composites (Filtek, Grandio, and SDR) ($p<0.05$), whereas no significant differences were found among the latter three materials ($p>0.05$).

The continuous fiber application resulted in a statistically significant overall effect across materials. The absence of a significant interaction indicates that the reinforcing effect of continuous fiber was consistent among the tested composites. In other words, the (positive) effect of continuous fiber incorporation did not depend on the composite.

In addition, the factor continuous fiber, a two level factor (with or without) was an overall significant factor, with marginal means of the continuous group being significantly higher ($p=0.024$).

Specimens without continuous fiber reinforcement exhibited brittle behavior, fracturing catastrophically into two separate pieces and being displaced from the loading area, indicating sudden failure once the maximum flexural strength was exceeded. In contrast, continuous fiber-reinforced specimens showed a more ductile response; they primarily bent and remained intact without complete separation, suggesting that the embedded fibers helped redistribute tensile stresses, bridging developing cracks, and delaying crack propagation. This change in failure mode implies that while ultimate load may be similar, fiber reinforcement improves energy absorption and damage tolerance under flexural loading, resulting in a safer, less catastrophic fracture pattern.

Conclusion

Flexural strength is a significant mechanical characteristic of dental composites, a helpful measure of material response under the multi-axial stresses encountered in the oral environment. Standardized three-point bending yields a good test technique for measuring and comparing materials, generating data of direct significance to clinical decision-making and choice of material (Chung et al. 1998). For conventional particulate-filled composites, flexural strength is dominated by filler content and type, resin matrix composition, and degree of conversion, with typical values typically between 80-140 MPa depending on test conditions and formulation (Chung et al. 1998). Fiber-reinforced composites represent a significant advance in dental materials, exhibiting much enhanced flexural properties compared to conventional counterparts (Chung et al. 1998). Through processes like stress transfer, crack deflection, and bridging effects, fiber reinforcement can enhance flexural strength by 25-200% depending on fiber orientation, type, and volume fraction. This improvement in mechanical properties extends the clinical use of resin-based materials to high-stress conditions previously requiring metal substructures, contributing to ongoing advances toward metal-free restorative methods.

While laboratory-measured flexural strength provides valuable data in material choice, clinicians must put these numbers into perspective against overall comprehensive mechanical characterization and pragmatic clinical considerations. The optimum material for an application takes mechanical properties in balance with handling qualities, aesthetic outcomes, and resistance to long-term challenges from the unfriendly conditions of the oral cavity. Since fiber-reinforced composites will keep changing based on research and development, their enhanced flexural performance can allow further development of their applications clinically, particularly in biomechanically demanding situations.

Across all experiments, material type and fiber reinforcement had a marked influence on flexural behavior and failure mode. The everX Flow, as a short fiber reinforced composite, consistently showed higher flexural strength and more favorable, non-catastrophic fracture patterns than the non fiber bulk-fill and nanohybrid composites, in line with previous evidence that short fiber–reinforced composites exhibit superior flexural performance and fracture toughness (Chung et al. 1998). Conventional bulk-fill and nanohybrid composites without additional reinforcement tended to fail abruptly with complete separation under three-point bending. In contrast, specimens reinforced with polyethylene fibers (Ribbond) demonstrated increased resistance to crack propagation, higher fracture or flexural strength in several prior flexural tests, and a transition from brittle, two-piece fractures to more ductile bending with partial or no separation, reflecting the ability of interlaced UHMWPE fibers to bridge cracks and redistribute tensile stresses. Overall, the combined findings support the use of fiber reinforced composites, and especially external Ribbond reinforcement, as an effective strategy to enhance the flexural performance and damage tolerance of resin based restorations.

Observations

Flexural testing revealed clear differences in how the specimens fractured depending on the presence of continuous fiber reinforcement. In the groups without continuous fiber reinforcement the bars typically exhibited abrupt, brittle failure, often separating into two or more pieces and occasionally projecting away from the loading area, indicating limited energy absorption before fracture. In contrast, specimens reinforced with continuous fiber reinforcement tended to remain partially or fully intact, showing more controlled bending and localized cracking rather than complete separation. This shift from catastrophic fragmentation to a more cohesive failure pattern suggests that the embedded fibers may have helped redistribute tensile stresses, bridge developing cracks, and modify the overall fracture behavior under flexural loading.

In the GrandioSo group (Fig. 14d), three-point flexural testing revealed a brittle, multi-fragment failure in the non-reinforced specimen (top), whereas the Ribbond-reinforced specimen (bottom) exhibited a more localized, two-piece fracture. This difference reflects the altered failure mode and improved flexural performance attributed to fiber reinforcement. Notably, the separation and brittleness were concentrated at the continuous fiber reinforcement interface.

In the Filtek groups, showing in figure 14c, distinct differences in fracture behavior were observed between specimens with and without Ribbond reinforcement. Bars without Ribbond showed a brittle response; they fractured quickly under flexural loading and separated into discrete segments, indicating limited capacity to absorb or redistribute tensile stresses. In contrast, Ribbond-reinforced Filtek specimens exhibited no visible brittleness or separation after testing. The composite remained well attached around the embedded fiber, and the bar generally stayed in one piece or

with only minimal cracking, suggesting that the Ribbond layer effectively constrained crack propagation and enhanced the structural integrity of the composite under flexural stress.

In the SDR Flow groups (14b), specimens without Ribbond reinforcement displayed a clearly brittle response, fracturing rapidly under flexural loading and separating into two distinct pieces. By contrast, the Ribbond-reinforced SDR Flow bars showed no obvious brittleness or separation after testing; the composite remained well attached around the fiber, and the specimen largely preserved its integrity with only minor visible cracking. This indicates that the Ribbond layer effectively stabilized the SDR Flow composite, limiting crack propagation and reducing catastrophic fragmentation during flexural loading.

In the everX groups (14a), flexural loading produced a distinctly brittle response in the specimens without Ribbond reinforcement, which fractured rapidly and separated into two clear segments with sharp fracture surfaces. In contrast, everX specimens reinforced with Ribbond tended to show a more controlled failure pattern, with the bar often remaining bridged at the fracture site and the composite still closely attached around the embedded fibers. This behavior suggests that, even in a short-fiber reinforced material such as everX, the additional continuous fiber helped distribute tensile stresses and limited complete separation of the specimen during bending.

Based on the stress strain curves obtained from the three-point bending test specimens reinforced with Ribbond demonstrated improved flexural performance compared with their non-reinforced counterparts (Fig.13). The Filtek + Ribbond group exhibited the highest peak load, reaching approximately 0.22 kN, which was substantially greater than the Filtek control group that peaked at roughly 0.10 kN. Similarly, reinforcement of everX Flow with Ribbond increased the maximum stress compared with everX Flow alone, although the difference was less pronounced than in the Filtek groups. In addition to higher peak stress, ribbon-reinforced specimens showed greater strain

before failure, indicating improved resistance to catastrophic fracture and enhanced energy absorption. In figure 13a, the graph presents the flexural strength of the different composite systems with and without the continuous fiber reinforcement. In most materials, incorporating the continuous polyethylene fiber increased flexural strength, with the most noticeable improvements observed in short fiber reinforced composite (everX flow) and regular composite (Filtek).

This suggests that fiber reinforcement can enhance load-bearing capacity, although the magnitude of improvement varies depending on the composite matrix. Overall, the incorporation of continuous fiber increased both the flexural strength and deformation capacity of the tested composite systems.

Tables and Figures

Material / Trade name	Manufacturer (city, country)	Type / description	Regular or fiber-reinforced
everX Flow	GC, Tokyo, Japan	Short E-glass fiber-reinforced, radiopaque bulk-fill flowable composite for dentin replacement and core build-up	Fiber-reinforced composite
SDR Flow+	Dentsply Sirona, Charlotte, NC, USA	Self-levelling bulk-fill flowable composite with low shrinkage stress for posterior restorations and base/liner applications	Regular composite
GrandioSO	VOCO, Cuxhaven, Germany	Universal nano-hybrid restorative composite with high filler content (~89 wt%)	Regular composite
Filtek Universal Restorative	3M, St. Paul, MN, USA	Light-cured universal nano-composite for anterior/posterior restorations	Regular composite

Material / Trade name	Manufacturer (city, country)	Type / description	Regular or fiber-reinforced
Ribbond / Ribbond Ultra	Ribbond Inc., Seattle, WA, USA	Woven ultra-high-molecular-weight polyethylene fiber ribbon for reinforcement	Fiber-reinforcing material
CLEARFIL SE Bond 2	Kuraray Noritake Dental Inc., Tokyo, Japan	Two-step self-etch, light-curing bonding agent used for adhesion to tooth structure	Adhesive (no fibers)
Paradigm LED curing light (or 3M ESPE LED unit)	3M ESPE, St. Paul, MN, USA	LED light-curing unit used to polymerize adhesive and composite according to manufacturers' instructions	Curing device

Table 1. Direct restorative materials and fiber reinforcement system used for flexural strength testing

Group	Material	Ribbond	Type	Description
G1	everX Flow	No	Short-fiber FRC	everX Flow alone
G2	everX Flow	Yes	Short-fiber FRC + continuous	everX Flow + Ribbond
G3	SDR Flow	No	Regular bulk-fill	SDR Flow alone
G4	SDR Flow	Yes	Regular + continuous	SDR Flow + Ribbond
G5	GrandioSO	No	Regular nano-hybrid	GrandioSO alone
G6	GrandioSO	Yes	Regular + continuous	GrandioSO + Ribbond
G7	Filtek	No	Regular universal	Filtek alone
G8	Filtek	Yes	Regular + continuous	Filtek + Ribbond

Table 2. Experimental groups categorized by composite material and presence or absence of fiber reinforcement.

Effect	F	p-value
Composite	11.06	0.000012
Continuous Fiber	5.40	0.024
Interaction	1.42	0.248

Table 3. Two-way ANOVA for the effect of composite type and continuous fiber reinforcement on flexural strength of all composite systems evaluated.

	EverX	SDR	Grandio	Filtek
EverX	—	<0.001*	<0.001*	<0.001*
SDR	<0.001*	—	0.42	0.78
Grandio	<0.001*	0.42	—	0.33
Filtek	<0.001*	0.78	0.33	—

Table 4. Pairwise comparisons among composite materials based on marginal means (averaged across continuous-fiber conditions), analyzed using Tukey's honestly significant difference (HSD) test following two-way ANOVA with no significant interaction. Values indicate adjusted p-values; significance level $\alpha = 0.05$. (*) indicates significant difference.

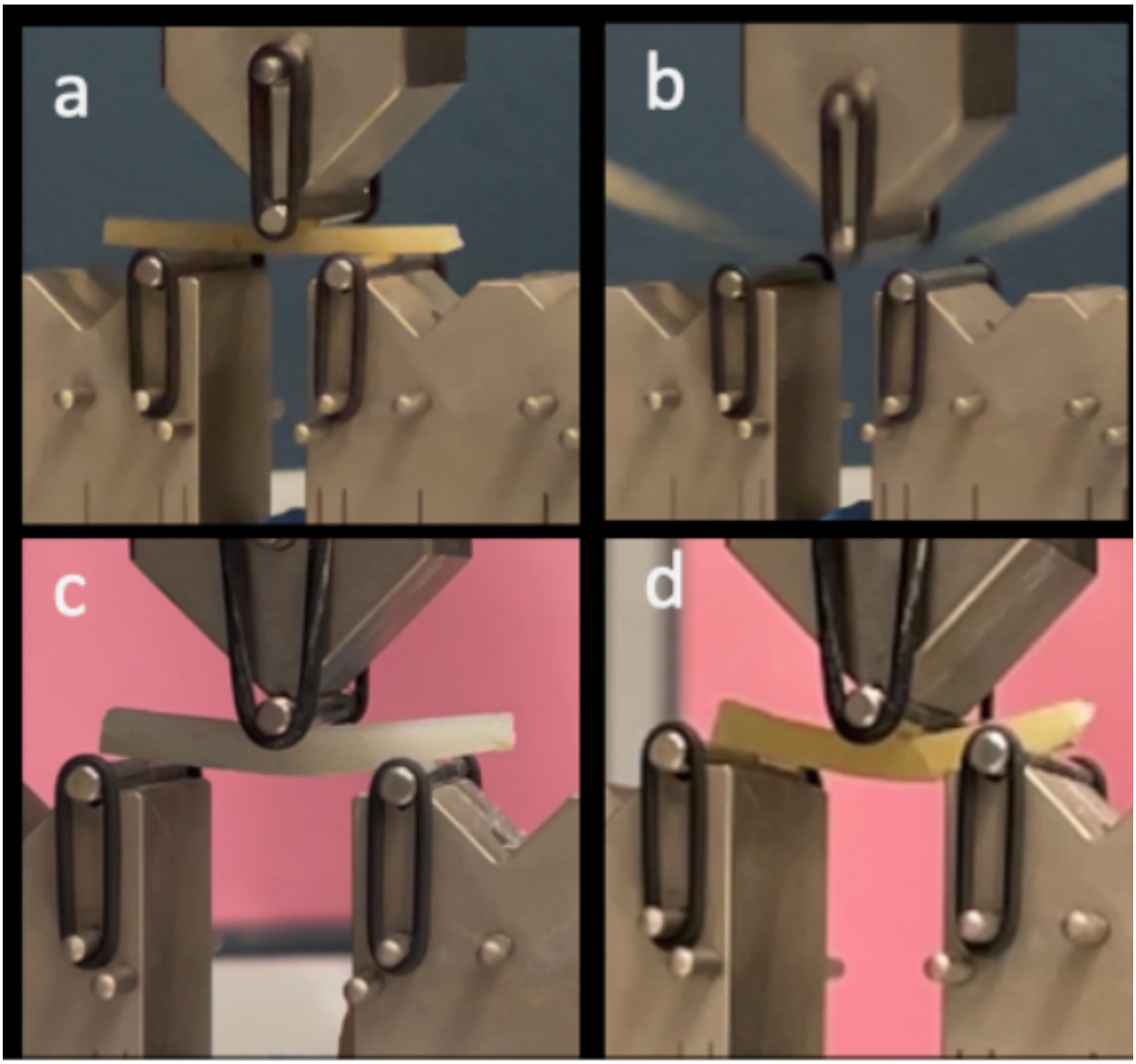

Figure 12. The three-point bending test setup to measure the flexural strength of each specimen; a) Pre-test for SDR with Ribbond specimen; b) SDR without Ribbond at the fracture moment; c) Mid-test image of a everX flow specimen with the bar bending but no visible crack in the specimen; d) mid-test image of a GrandioSo specimen. The visible crack indicates the failure pattern.

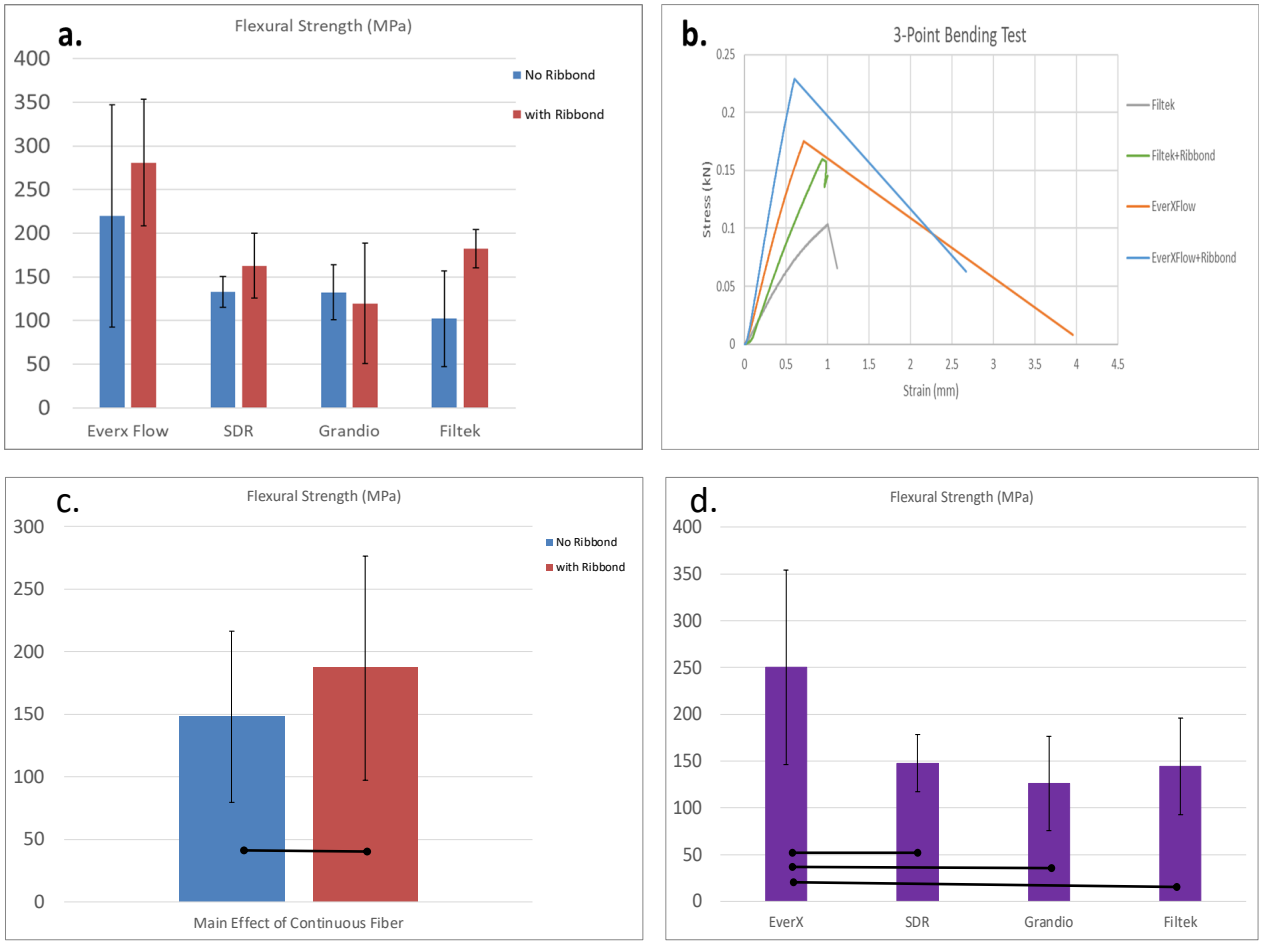

Figure 13. a. The graph presents the flexural strength of the different composite systems with and without the continuous fiber reinforcement. b. Stress–strain curves generated from three point bending tests performed on an Instron universal testing machine. The graph compares the flexural response of Filtek and everX Flow and their corresponding continuous fiber (Ribbond) reinforced groups. c. Post-hoc pair-wise comparison for the main effect of continuous fiber. Horizontal bar presents significant difference ($p<0.05$). d. Post-hoc pair-wise comparison for the main effect of the composite type. Horizontal bar presents significant difference ($p<0.01$).

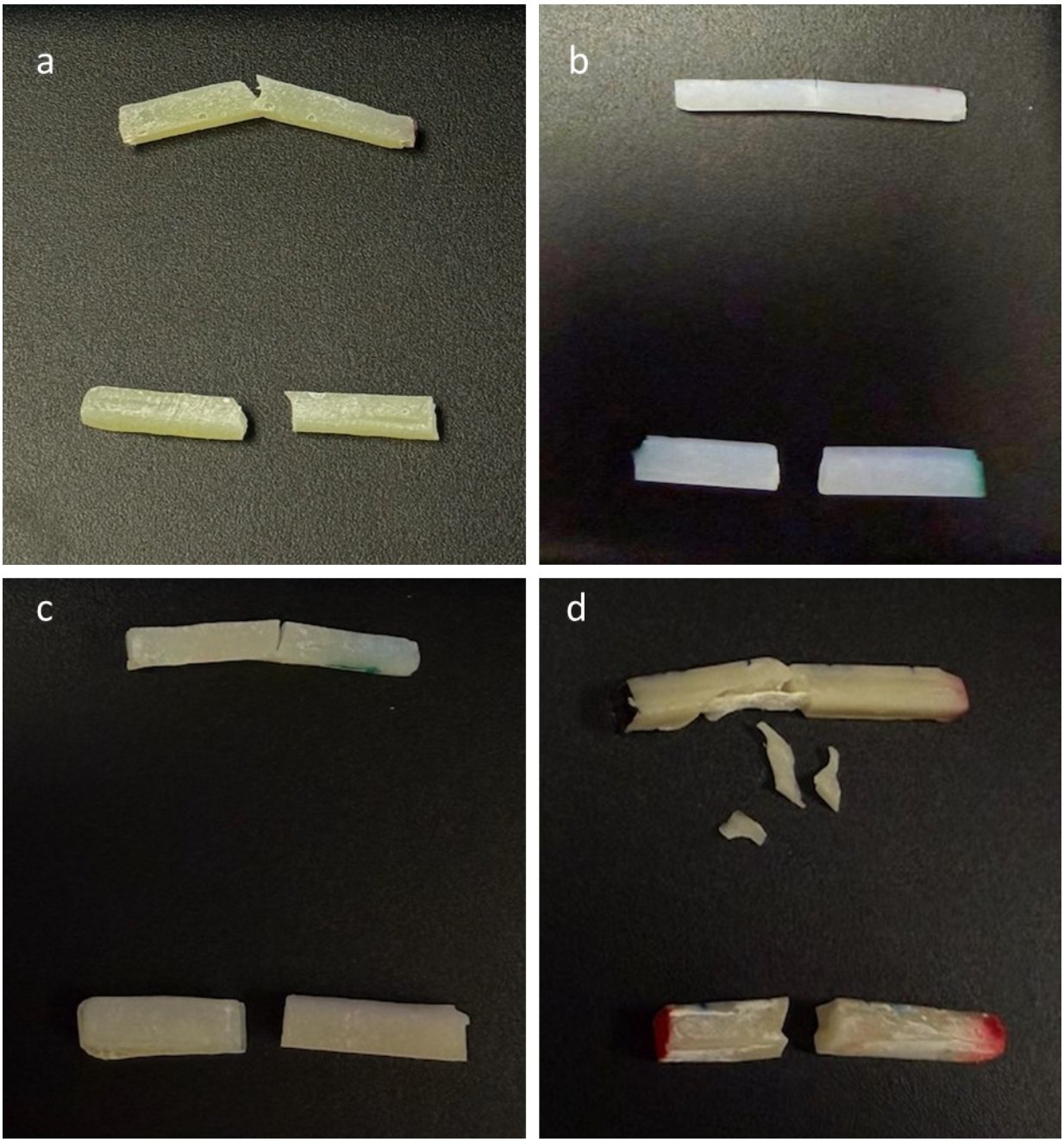

Figure 14. Typical fracture mode for the 3-point bending test bar specimens. In all panel, the top specimen is with incorporation of Ribbond and the bottom bar is the material without fiber. a: everX Flow; b: SDR Flow; c: Filtek; d: GrandioSo.

Chapter 4: Discussion and Future Directions

Collectively, the following conclusions were drawn from this series of experiments:

1. Incorporation of a continuous UHMWPE fiber improved the cavity-floor adaptation of all tested composite materials.
2. Short-fiber–reinforced composites exhibited shrinkage stress development comparable to the particulate flowable composite; however, they still benefitted from the addition of a continuous UHMWPE fiber.
3. The addition of a continuous UHMWPE fiber enhanced the flexural strength of all tested flowable composites.
4. The short-fiber–reinforced composite demonstrated higher flexural strength than the particulate flowable composite.
5. The combination of short E-glass fibers with a continuous UHMWPE fiber yielded the most promising overall performance.

Future research should build on these findings by optimizing fiber position, architecture, and pretreatment to maximize stress transfer at the fiber–resin interface and to further reduce catastrophic failure under flexural loading. Students continuing this work could: systematically vary Ribbond location (tension surface versus central versus multiple layers) and orientation; compare different fiber types (polyethylene versus various glass or novel fibers) within the same composite systems; incorporate thermo-mechanical cycling, fatigue loading, and aging protocols to better simulate intraoral conditions; combine mechanical testing with fractographic and microscopic analysis to correlate failure patterns with microstructural features and look into various

surface treatments to improve integration of UHMWPE fiber into the methacrylate-based composites.

Over the next 10 years, the field of fiber reinforced restorative materials is likely to move toward bioinspired, highly tough composites that integrate short fibers, woven, or 3D fiber networks, and smart resin matrices designed for improved fracture toughness, fatigue resistance, and repairability. Expanded clinical evidence on short fiber reinforced composites such as everX Flow, together with new generations of high modulus, high adhesion fibers, will likely make fiber reinforced restorations a routine option for managing large posterior defects, minimally invasive on-lays, and splinting or reinforcement of structurally compromised teeth. Clinically, this technique uses continuous fiber to bridge and reinforce weakened cusps, distribute functional and shrinkage stresses more evenly, and may reduce crack propagation and marginal breakdown compared with a conventional composite placed without fiber reinforcement (Fig. 16)

Throughout the course of my research, I directly observed several practical difficulties associated with the use of fiber reinforcement in resin-based composite restorations. Despite the mechanical advantages offered by fiber reinforcement, several important limitations warrant consideration. The addition of fibers can increase the technique sensitivity of the procedure, as successful reinforcement depends heavily on precise placement, correct orientation, and thorough impregnation of the fibers within the resin matrix. Systems such as polyethylene-based continuous fiber like Ribbond require meticulous handling and complete resin wetting to achieve reliable adhesion. When fibers are inadequately impregnated or positioned incorrectly, the result may be diminished reinforcement efficiency and the introduction of internal defects. These additional steps also extend clinical time and add procedural complexity compared with conventional composite restorations.

A further limitation involves the quality of the fiber–matrix interface. Some reinforcing fibers particularly ultra-high-molecular-weight polyethylene are chemically inert and exhibit limited chemical interaction with methacrylate-based resins. Weak interfacial bonding increases the risk of fiber–matrix debonding under functional loading, which compromises the intended reinforcement effect. Inadequate adaptation of the fiber layer may also create voids or localized stress concentrations within the restoration, potentially undermining its structural integrity. From an esthetic standpoint, fibers placed too close to the surface can alter the optical properties of the composite, affecting translucency and overall appearance.

Although numerous in vitro studies demonstrate improvements in fracture resistance and crack propagation control, long-term clinical evidence remains comparatively limited for several fiber-reinforced restorative approaches. Additional well-designed clinical studies are needed to confirm their durability, performance, and predictability over time.

Figure 15. The clinical sequence shows replacement of a defective amalgam restoration with a bonded, fiber reinforced composite using Ribbond. The parts a and b represent a fractured tooth and its restoration material (amalgam).

c. After removal of the old amalgam and caries, the teeth were isolated with rubber dam, and the proximal walls were rebuilt using sectional matrices and a standard adhesive protocol so that a well-defined cavity with supported margins was obtained. Precut Ribbond fiber strips were saturated with bonding resin and adapted across the pulpal floor and into the proximal box, then light cured to create an internal fiber framework. d. The cavity was subsequently incrementally restored with resin composite over the Ribbond, followed by occlusal adjustment and polishing to achieve proper anatomy and contacts.

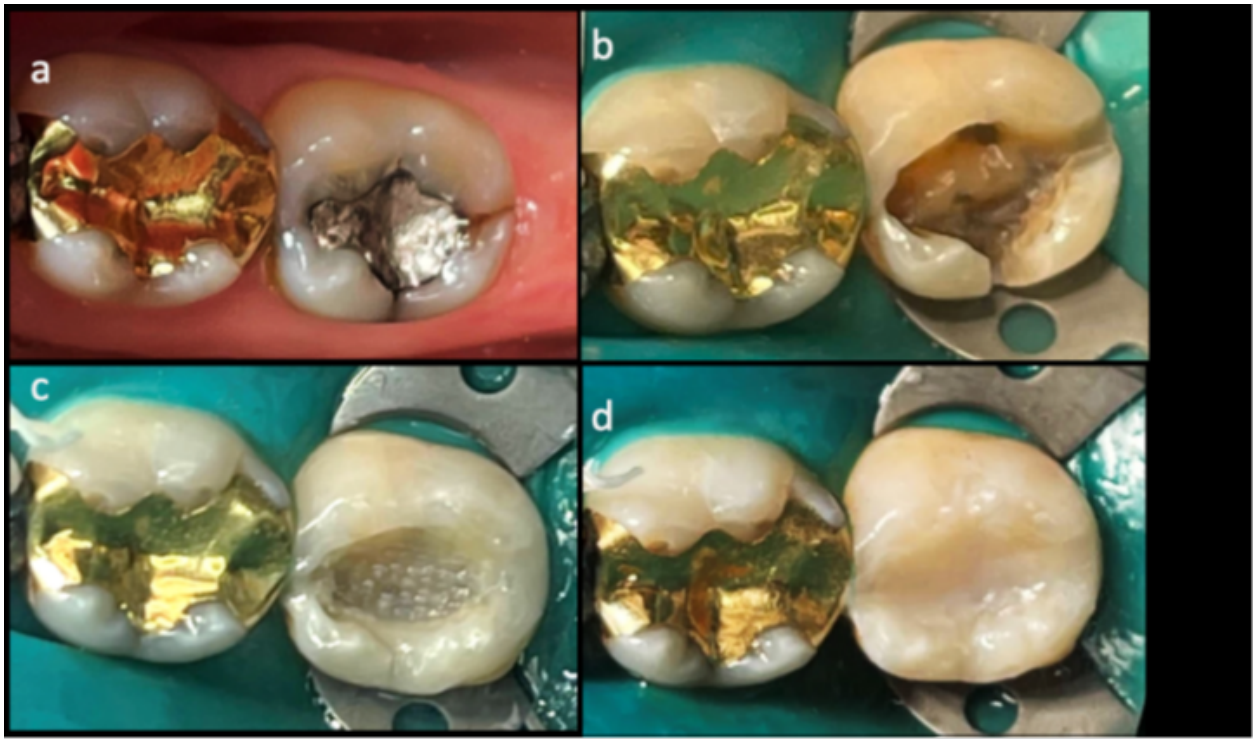

Figure 16. Top left panel: a. Clinical presentation of a lower second molar with cold and bite sensitivity. Note the orientation of distal marginal ridge and lingual surface cracks. Joining mesio-distal cracks under the existing restoration is suspected. b. After anesthesia and rubber dam placement, the amalgam restoration was removed, the cracks were chased to the gingival level and rounded. c. After bonding with an antibacterial fluoride-releasing 2-step self etch, the circumferentiak walls were completer with particulate composite, then a piece of 4 mm wide Ribbond was cut to the length. The fiber was placed over the pulpal floor and up the axial walls after wetting with the bonding agent and a flowable composite as the embedding composite. d. Pre-finishing restoration completed with incremental placement of the hybrid restorative composite.

(Image from clinical work by Dr. Sadr, at University of Washington)

List of Abbreviations

- ASTM – American Society for Testing and Materials
- CAD-CAM – Computer-Aided Design / Computer-Assisted Manufacturing
- C-factor – Configuration factor (ratio of bonded to unbonded surfaces)
- CPC – Clearfil Photo Core
- DC-R – Degree of Conversion Ratio (bottom-to-top)
- FDP – Fixed Dental Prosthesis
- FRC – Fiber-Reinforced Composite
- GIC – Glass Ionomer Cement
- ISO – International Organization for Standardization
- LED – Light-Emitting Diode
- MTBS – Microtensile Bond Strength
- OCT – Optical Coherence Tomography
- RBC – Resin-Based Composite
- SDR – SDR Flow bulk-fill composite
- SFA% – Sealing Floor Area Percentage
- SS-OCT – Swept-Source Optical Coherence Tomography
- UHMWPE – Ultra-High-Molecular-Weight Polyethylene
- VS% – Volumetric Shrinkage Percentage

References

Abdul-Monem, M. M., El-Gayar, I. L., & Al-Abbassy, F. H. (2016). Effect of aging on the flexural strength and fracture toughness of a fiber reinforced composite resin versus two nanohybrid composite resins. Alex Dent J, 41, 328–335.

Aguiar, F. H., Ajudarte, K. F., & Lovadino, J. R. (2002). Effect of light curing modes and filling techniques on microleakage of posterior resin composite restorations. Oper Dent, 27(6), 557–562.

Alani, A. H., & Toh, C. G. (1997). Detection of microleakage around dental restorations: a review. Oper Dent, 22(4), 173–185.

Alleman, D. S., & Deliperi, S. (2013). Adhesive dentistry: 2013 and into the future. Compend Contin Educ Dent, 34(9), 698–699.

Alqudaihi, F. S., et al. (2019). Comparison of internal adaptation of bulk-fill and increment-fill resin composite materials. Oper Dent, 44(1), E32–E44.

Aquilino, S. A., & Caplan, D. J. (2002). Relationship between crown placement and the survival of endodontically treated teeth. J Prosthet Dent, 87(3), 256–263.

Balto, H., Al-Nazhan, S., Al-Mansour, K., Al-Otaibi, M., & Siddiqu, Y. (2005). Microbial leakage of Cavit, IRM, and Temp Bond in post-prepared root canals using two methods of gutta-percha removal: an in vitro study. J Contemp Dent Pract, 6(3), 53–61.

Belli, R., et al. (2009). In vitro wear gap formation of self adhesive resin cements: a CLSM evaluation. J Dent, 37(12), 984–993.

Belli, S., Erdemir, A., Ozcopur, M., & Eskitascioglu, G. (2005). The effect of fiber insertion on fracture resistance of root filled molar teeth with MOD preparations restored with composite. Int Endod J, 38(2), 73–80.

Braga, R. R., & Ferracane, J. L. (2002). Contraction stress related to degree of conversion and reaction kinetics. J Dent Res, 81(2), 114–118.

Breschi, L., et al. (2003). Morphological study of resin-dentin bonding with TEM and in-lens FESEM. Am J Dent, 16(4), 267–274.

Calheiros, F. C., Pfeifer, C. S., Brandão, L. L., Agra, C. M., & Ballester, R. Y. (2013). Flexural properties of resin composites: influence of specimen dimensions and storage conditions. Dent Mater J, 32, 228–232.

Callister, W. D., & Rethwisch, D. G. (2018). Materials Science and Engineering: An Introduction (10th ed.). John Wiley & Sons.

Caussin, E., Izart, M., Ceinos, R., Attal, J. P., Beres, F., & François, P. (2024). Advanced material strategy for restoring damaged endodontically treated teeth: A comprehensive review. Materials (Basel), 17, 15.

Chung, K., Lin, T., & Wang, F. (1998). Flexural strength of a provisional resin material with fibre addition. J Oral Rehabil, 25(3), 214–217. https://doi.org/10.1046/j.1365-2842.1998.00201.

Chyz, G. T. (2010). Restoration of an “at risk” tooth: replacing an old amalgam with a fiber mesh and a nano composite [Internet]. Seattle (WA): Ribbond Inc.; c2010 [cited 2026 Feb 22]. Retrieved January 2, 2026, from : https://ribbond.com/pdf/compositerestorations/Chyz-RestorationAtRiskTooth.pdf

Coldebella, C. R., Melo Ribeiro, M., Paranhos, C., Buarque, T., Buarque, E., Furuse, C., et al. (2009). Nanocomposite used in dentistry. Eur Cells Mater, 10, 10–19.

Cramer, N. B., Stansbury, J. W., & Bowman, C. N. (2011). Recent advances and developments in composite dental restorative materials. J Dent Res, 90(4), 402–416.

Davidson, C. L. (1986). Resisting the curing contraction with adhesive composites. J Prosthet

Dent, 55(4), 446–447.

de Menezes, A. J. O., do Nascimento Barbosa, L., Leite, J. V. C., Barbosa, L. M. M., Montenegro, R. V. F., Dantas, R. V. F., de Souza, G. M., de Andrade, A. K. M., & Lima, R. B. W. (2024). Clinical outcomes of bulk fill resin composite restorations: A 10 year mapping review and evidence gap map. J Esthet Restor Dent.

de Toubes, K. M. S., Soares, C. J., Soares, R. V., Côrtes, M. I. S., Tonelli, S. Q., Bruzinga, F. F. B., & Silveira, F. F. (2022). The correlation of crack lines and definitive restorations with the survival and success rates of cracked teeth: A long term retrospective clinical study. J Endod, 48(2), 190–199.

Deliperi, S. (2008). Direct fiber reinforced composite restoration in an endodontically treated molar: a three year case report. Oper Dent, 33(2), 209–214.

Deliperi, S., Alleman, D., & Rudo, D. (2017). Stress reduced direct composites for the restoration of structurally compromised teeth: Fiber design according to the “wallpapering” technique. Oper Dent, 42(3), 233–243.

Dietrich, T., Lösche, A. C., Lösche, G. M., & Roulet, J. F. (1999). Marginal adaptation of direct composite and sandwich restorations in Class II cavities with cervical margins in dentine. J Dent, 27(2), 119–128.

Drummond, J. L. (2009). Degradation, fatigue, and failure of resin dental composite materials. J Dent Res, 87, 710–719.

El Damanhoury, H. M., & Platt, J. A. (2014). Polymerization shrinkage stress kinetics and related properties of bulk fill resin composites. Oper Dent, 39(4), 374–382.

Escobar, L. B., Pereira da Silva, L., & Manarte Monteiro, P. (2023). Fracture resistance of fiber reinforced composite restorations: A systematic review and meta analysis. Polymers (Basel), 15,

18.

Espigares, J., Sadr, A., Hamba, H., Shimada, Y., Otsuki, M., Tagami, J., & Sumi, Y. (2015). Assessment of natural enamel lesions with optical coherence tomography in comparison with microfocus x ray computed tomography. J Med Imaging (Bellingham), 2(1), 014001.

Espinoza, K., Hayashi, J., Shimada, Y., Tagami, J., & Sadr, A. (2021). Optical coherence tomography for patients with developmental disabilities: A preliminary study. Sensors (Basel), 21(23), 7940.

Farman, A., Horsley, B., Warr, E., Ianke, J., & Hood, H. (2003). Outcomes of digital X ray mini panel examinations for patients having mental retardation and developmental disability. Dentomaxillofac Radiol, 32(1), 15–20.

Feng, L., et al. (2010). Formation of gaps at the filler resin interface induced by polymerization contraction stress: Gaps at the interface. Dent Mater, 26(8), 719–729.

Fernández, E., Díaz, L., Bersezio, C., Martín, J., Cabello, R. & Angel P (2026). Efficacy of Short Fiber-Reinforced Composite Resins in MOD and Endodontically Treated Posterior Teeth: A Systematic Review. J Esthet Restor Dent, 38(2):268-286.

Ferracane, J. L. (2011). Resin composite – State of the art. Dent Mater, 27(1), 29–38.

Ferracane, J. L. (2024). A historical perspective on dental composite restorative materials. J Funct Biomater, 15(7), 173.

Fokkinga, W. A., Kreulen, C. M., Vallittu, P. K., & Creugers, N. H. (2004). A structured analysis of in vitro failure loads and failure modes of fiber, metal, and ceramic post and core systems. Int J Prosthodont, 17(4), 476–482.

Fousekis, E., Lolis, A., Marinakis, E., Oikonomou, E., Foros, P., Koletsi, D., & Eliades, G. (2023). Short fiber reinforced composite resins as post and core materials for endodontically

treated teeth: A systematic review and meta analysis of in vitro studies. J Prosthet Dent.

Gabriele, M. L., et al. (2011). Optical coherence tomography: history, current status, and laboratory work. Invest Ophthalmol Vis Sci, 52(5), 2425–2436.

Gagnier, J. J., Kienle, G., Altman, D. G., Moher, D., Sox, H., & Riley, D. (2013). The CARE Guidelines: Consensus based clinical case reporting guideline development. Glob Adv Health Med, 2(5), 38–43.

Ganesh, M., & Tandon, S. (2006). Versatility of Ribbond in contemporary dental practice. Trends Biomater Artif Organs, 20(1), 53–58.

Garoushi, S., Tanner, J., Vallittu, P. K., & Lassila, L. (2012). Preliminary clinical evaluation of short fiber reinforced composite resin in posterior teeth: 12 months report. Open Dent J, 6, 41–45.

Garoushi, S., Vallittu, P. K., & Lassila, L. V. (2008). Fracture toughness, compressive strength and load bearing capacity of short glass fiber reinforced composite resin. Chin J Dent Res, 11, 14–18.

Garoushi, S., et al. (2009). Continuous and short fiber reinforced composite in root post core system of severely damaged incisors. Open Dent J, 3, 36–41.

Glassman, P., Caputo, A., Dougherty, N., Lyons, R., Messieha, Z., Miller, C., Peltier, B., & Romer, M. (2009). Special Care Dentistry Association consensus statement on sedation, anesthesia, and alternative techniques for people with special needs. Spec Care Dentist, 29(1), 2–8.

Gordon, S. M., Dionne, R. A., & Snyder, J. (1998). Dental fear and anxiety as a barrier to accessing oral health care among patients with special health care needs. Spec Care Dentist, 18(2), 88–92.

Hariri, I., Sadr, A., Shimada, Y., Tagami, J., & Sumi, Y. (2012). Effects of structural orientation

of enamel and dentin on light attenuation and local refractive index: an optical coherence tomography study. J Dent, 40(5), 387–396.

Hayashi, J., Espigares, J., Takagaki, T., Shimada, Y., Tagami, J., Numata, T., Chan, D., & Sadr, A. (2019). Real time in depth imaging of gap formation in bulk fill resin composites. Dent Mater, 35(4), 585–596.

Heintze, S., Henrich, A., Bürgers, R., Handl, G., & Rosentritt, M. (2010). Investigation of mechanical behavior of dental resin composite after artificial aging for 2 years. Dent Mater, 26, 412–419.

International Organization for Standardization. ISO 4049/2000 – Dentistry – Polymer based filling, restorative and luting materials. Switzerland: ISO; 2000.

Karlsson, L. (2010). Caries detection methods based on changes in optical properties between healthy and carious tissue. Int J Dent, 2010, 270729.

Keulemans, F., Garoushi, S., & Lassila, L. (2017). Fillings and core build ups. In P. Vallittu & M. Özcan (Eds.), A Clinical Guide to Principles of Fiber Reinforced Composites (FRCs) in Dentistry (pp. 131–163). Duxford: Woodhead Publishing.

Khan, S. I., Anupama, R., Deepalakshmi, M., & Kumar, K. S. (2013). Effect of two different types of fibers on the fracture resistance of endodontically treated molars restored with composite resin. J Adhes Dent, 15(2), 167–171.

Kitasako, Y., Sadr, A., Shimada, Y., Ikeda, M., Sumi, Y., & Tagami, J. (2019). Remineralization capacity of carious and non carious white spot lesions: Clinical evaluation using ICDAS and SS OCT. Clin Oral Investig, 23(2), 863–872.

Klingberg, G., & Broberg, A. G. (2007). Dental fear/anxiety and dental behavior management problems in children and adolescents: a review of prevalence and concomitant psychological

factors. Int J Paediatr Dent, 17(6), 391–406.

Leal, T. A. C., et al. (2021). Physiologic and behavioral signs during a dental appointment in children and teenagers with cerebral palsy: A comparative cross sectional study. Eur Arch Paediatr Dent, 22(2), 181–186.

Luong, M. N., Shimada, Y., Araki, K., Yoshiyama, M., Tagami, J., & Sadr, A. (2020). Diagnosis of occlusal caries with dynamic slicing of 3D optical coherence tomography images. Sensors (Basel), 20(6), 1659.

Magne, P., Boff, L. L., Oderich, E., & Cardoso, A. C. (2012). CAD/CAM adhesive restoration of molars with a compromised cusp: effect of fiber reinforced immediate dentin sealing and cusp overlap on fatigue strength. J Esthet Restor Dent, 24(2), 135–146.

Martin, M. D., Kinoshita Byrne, J., & Getz, T. (2002). Dental fear in a special needs clinic population of persons with disabilities. Spec Care Dentist, 22(3), 99–102.

Masouras, K., Silikas, N., & Watts, D. C. (2008). Correlation of filler content and elastic properties of resin composites. Dent Mater, 24, 932–939.

Mata, E. G. (2011). Relationship between filler content and selected mechanical properties of six microhybrid composites. J Dent, 26, 519–525.

Maxwell, E. H., Braly, B. V., & Eakle, W. S. (1986). Incompletely fractured teeth – a survey of endodontists. Oral Surg Oral Med Oral Pathol, 61(1), 113–117.

Medina Tirado, J. I., Nagy, W. W., Dhuru, V. B., & Ziebert, A. J. (2012). The effect of thermocycling on the fracture toughness and hardness of core buildup materials. J Prosthet Dent, 86, 474–480.

Meyenberg, K. (2013). The ideal restoration of endodontically treated teeth – structural and esthetic considerations: a review of the literature and clinical guidelines for the restorative

clinician. Eur J Esthet Dent, 8(2), 238–268.

Nakagawa, H., Sadr, A., Shimada, Y., Tagami, J., & Sumi, Y. (2013). Validation of swept source optical coherence tomography (SS OCT) for the diagnosis of smooth surface caries in vitro. J Dent, 41(1), 80–89.

Nelson, L. P., et al. (2011). Unmet dental needs and barriers to care for children with significant special health care needs. Pediatr Dent, 33(1), 29–36.

Ni, J., Xu, L., Lin, Y., Lai, D., & Huang, X. (2023). Effects of different full coverage designs and materials on crack propagation in first mandibular molar: an extended finite element method study. Front Bioeng Biotechnol, 11, 1222060.

Opdam, N. J., Roeters, J. J., Loomans, B. A., & Bronkhorst, E. M. (2008). Seven year clinical evaluation of painful cracked teeth restored with a direct composite restoration. J Endod, 34(7), 808–811.

Panitvisai, P., & Messer, H. H. (1995). Cuspal deflection in molars in relation to endodontic and restorative procedures. J Endod, 21(2), 57–61.

Park, J. G., et al. (2009). Water sorption and dynamic mechanical properties of dentin adhesives with a urethane based multifunctional methacrylate monomer. Dent Mater, 25(12), 1569–1575.

Peltier, B. (2009). Psychological treatment of fearful and phobic special needs patients. Spec Care Dentist, 29(1), 51–57.

Pitts, N. B., Hamood, S. S., Longbottom, C., & Rimmer, P. A. (1991). The use of bitewing positioning devices in children's dentistry. Dentomaxillofac Radiol, 20(3), 121–126.

Ploumaki, A., Bilkhair, A., Tuna, T., Stampf, S., & Strub, J. R. (2013). Success rates of prosthetic restorations on endodontically treated teeth; a systematic review after 6 years. J Oral Rehabil, 40(8), 618–630.

Randall, R. C., & Wilson, N. H. F. (1999). Clinical testing of restorative materials: some historical landmarks. J Dent, 27(8), 543–550.

Reeh, E. S., Messer, H. H., & Douglas, W. H. (1989). Reduction in tooth stiffness as a result of endodontic and restorative procedures. J Endod, 15(11), 512–516.

Sadr, A., Bakhtiari, B., Hayashi, J., Luong, M. N., Chen, Y. W., Chyz, G., Chan, D., & Tagami, J. (2020). Effects of fiber reinforcement on adaptation and bond strength of a bulk fill composite in deep preparations. Dent Mater, 36(4), 527–534.

Sadr, A., Shimada, Y., et al. (2011). Swept source optical coherence tomography for quantitative and qualitative assessment of dental resin composite restorations. Proc SPIE, 7884, 78840C.

Salmasi, A., Harrison, R., & Brondani, M. A. (2015). They stole her teeth! An exploration of adults with developmental disability experiences with dental care. Spec Care Dentist, 35(5), 221–228.

Selvaraj, H., Krithikadatta, J., Shrivastava, D., Onazi, M. A. A., Algarni, H. A., Munaga, S., Hamza, M. O., Saad AlFridy, T., Teja, K. V., Janani, K., Alam, M. K., & Srivastava, K. C. (2023). Fracture resistance of endodontically treated posterior teeth restored with fiber reinforced composites – a systematic review. BMC Oral Health, 23(1), 566.

Shah P, Panjeta T, Mahla N, Sakina Z, Fernandes G. Current advances in adhesive dentistry: a mini review. IOSR J Pharm Biol Sci. 2023;18(2):46–49. doi:10.9790/3008-1802014649.

Shimada, Y., Nakagawa, H., Sadr, A., Wada, I., Nakajima, M., Nikaido, T., Otsuki, M., Tagami, J., & Sumi, Y. (2014). Non-invasive cross-sectional imaging of proximal caries using swept source optical coherence tomography (SS OCT) in vivo. J Biophotonics, 7(7), 506–513.

Shimada, Y., Sadr, A., Sumi, Y., & Tagami, J. (2015). Application of optical coherence tomography (OCT) for diagnosis of caries, cracks, and defects of restorations. Curr Oral Health

Rep, 2(2), 73–80.

Shivanna, V., & Gopeshetti, P. B. (2012). Fracture resistance of endodontically treated teeth restored with composite resin reinforced with polyethylene fibres. Endodontology, 24(1), 73–79.

Soares, C. J., Santana, F. R., Silva, N. R., Preira, J. C., & Pereira, C. A. (2007). Influence of the endodontic treatment on mechanical properties of root dentin. J Endod, 33(5), 603–606.

Soares, C. J., Soares, P. V., de Freitas Santos Filho, P. C., Castro, C. G., Magalhaes, D., & Versluis, A. (2008). The influence of cavity design and glass fiber posts on biomechanical behavior of endodontically treated premolars. J Endod, 34(8), 1015–1019.

Soares de Toubes, K. M., Moreira Maia, L., Cota Goulart, L., de Freitas Teixeira, T., Silva, N., Isaías Seraidarian, P., & Silveira, F. F. (2020). Optimization of results for cracked teeth using CAD CAM system: a case series. Iran Endod J, 15(1), 57–63.

Soto Cadena, S. L., Zavala Alonso, N. V., Cerda Cristerna, B. I., & Ortiz Magdaleno, M. (2023). Effect of short fiber reinforced composite combined with polyethylene fibers on fracture resistance of endodontically treated premolars. J Prosthet Dent, 129(4), 598.e1.

Sugiura, M., Kitasako, Y., Sadr, A., Shimada, Y., Sumi, Y., & Tagami, J. (2016). White spot lesion remineralization by sugar free chewing gum containing bio available calcium and fluoride: A double blind randomized controlled trial. J Dent, 54, 86–91.

Suzuki, T., Kyoizumi, H., Finger, W. J., Kanehira, M., Endo, T., Utterodt, A., et al. (2011). Resistance of nanofill and nanohybrid resin composites to toothbrush abrasion with calcium carbonate slurry. Dent Mater J, 28, 708–716.

Taha, D., et al. (2018). Fracture resistance and failure modes of polymer infiltrated ceramic endocrown restorations with variations in margin design and occlusal thickness. J Prosthodont Res, 62(3), 293–297.

Tang, W., Wu, Y., & Smales, R. J. (2010). Identifying and reducing risks for potential fractures in endodontically treated teeth. J Endod, 36(4), 609–617.

Tekçe, N., Pala, K., Tuncer, S., Demirci, M., & Serim, M. E. (2017). Influence of polymerisation method and type of fibre on fracture strength of endodontically treated teeth. Aust Endod J, 43(3), 115–122.

Ueno, T., Shimada, Y., Matin, K., Zhou, Y., Wada, I., Sadr, A., Sumi, Y., & Tagami, J. (2016). Optical analysis of enamel and dentin caries in relation to mineral density using swept source optical coherence tomography. J Med Imaging (Bellingham), 3(3), 035507.

Vallittu, P. K. (1996). A review of fiber reinforced denture base resins. J Prosthodont, 5(4), 270–276.

Van Hilsen, Z., & Jones, R. S. (2013). Comparing potential early caries assessment methods for teledentistry. BMC Oral Health, 13, 16.

Van Noort, R. (2007). Introduction to dental materials (3rd ed., pp. 99–126). London, UK: Elsevier.

Vatankhah, M., Ashraf, H., Jamalian, F., Talebi, S., Akbarzadeh Baghban, A., Khosravi, K., & Zargar, N. (2024). Success of nonsurgical endodontically treated posterior teeth with complex restorative/prosthodontic treatments: a retrospective study. Iran Endod J, 19(4), 263–269.

Visser, H. J., Brandt, P. D., & de Wet, F. A. (2014). Fracture strength of cusp replacing fibre strengthened composite restorations. SADJ, 69(5), 202, 204–207.

Waldman, H. B., & Perlman, S. P. (2012). Ensuring oral health for older individuals with intellectual and developmental disabilities. J Clin Nurs, 21(5–6), 909–913.

Wang, R., Habib, E., & Zhu, X. X. (2018). Evaluation of the filler packing structures in dental resin composites: From theory to practice. Dent Mater, 34(7), 1014–1023.

Wierichs, R. J., Kramer, E. J., Wolf, T. G., Naumann, M., & Meyer Lueckel, H. (2019). Longevity of composite build ups without posts – 10 year results of a practice based study. Clin Oral Investig, 23(3), 1435–1442.

Wilson, N. J., Lin, Z., Villarosa, A., Lewis, P., Philip, P., Sumar, B., & George, A. (2019). Countering the poor oral health of people with intellectual and developmental disability: a scoping literature review. BMC Public Health, 19, 1530.

Yoshikawa, T; Arakawa, M1. Effects of C-factor on dentin bonding using various adhesive systems. Niger J Clin Pract 25(3):p 255-260, March 2022. | DOI: 10.4103/njcp.njcp_1364_21

Zain, E., Zakian, C., & Chew, H. (2018). Influence of the loci of non cavitated fissure caries on its detection with optical coherence tomography. J Dent, 71, 31–37.

Zaitsev, V., Matveyev, A. L., Matveev, L. A., Gelikonov, G. V., Baum, O. I., Omelchenko, A. I., Shabanov, D. V., Sovetsky, A. A., Yuzhakov, A. V., Fedorov, A. A., et al. (2019). Revealing structural modifications in thermomechanical reshaping of collagenous tissues using optical coherence elastography. J Biophotonics, 12(3), e201800250.

List of Figures

Chapter 4

Figure 15. Clinical sequence showing replacement of a defective amalgam restoration with a bonded, fiber-reinforced composite using Ribbond.

Figure 16. Clinical case of cracked lower second molar restored using a continuous fiber reinforcement technique.

List of Tables

Chapter 2

Chapter 3